Article

Cell

Limbic Neurons Shape Sex Recognition and Social Behavior in Sexually Naive Males

Graphical Abstract

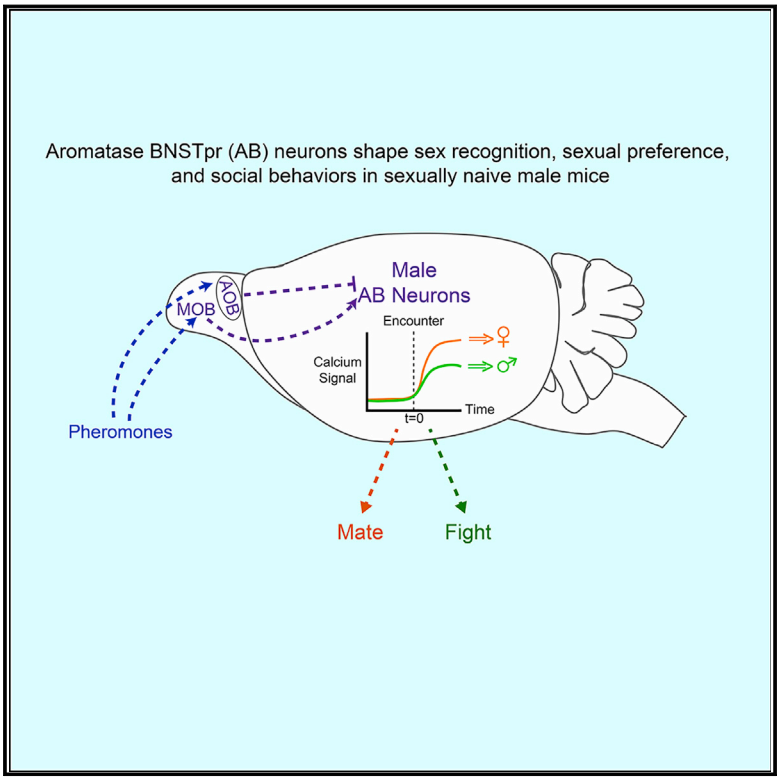

Authors

Daniel W. Bayless, Taehong Yang, Matthew M. Mason, Albert A.T. Susanto, Alexandra Lobdell, Nirao M. Shah

Correspondence

nirao@stanford.edu

In Brief

Aromatase-expressing BNSTpr neurons govern sex recognition and social behavior in naive male mice.

Highlights

- In sexually naive males, activity of AB neurons encodes sex of conspecifics
- Male AB neurons are required for sexual preference, mating, and aggression
- Activation of male AB neurons promotes male-male sexual behavior
- Females use other, non-AB neurons for sex recognition, mating, and maternal care

Bayless et al., 2019, Cell *176*, 1190–1205
February 21, 2019
https://doi.org/10.1016/j.cell.2018.12.041

CellPress

Cell

Article

Limbic Neurons Shape Sex Recognition and Social Behavior in Sexually Naive Males

Daniel W. Bayless,[1] Taehong Yang,[1] Matthew M. Mason,[1] Albert A.T. Susanto,[1] Alexandra Lobdell,[1] and Nirao M. Shah[1,2,3,*]

[1]Department of Psychiatry and Behavioral Sciences, Stanford University, Stanford, CA 94305, USA
[2]Department of Neurobiology, Stanford University, Stanford, CA 94305, USA
[3]Lead Contact
*Correspondence: nirao@stanford.edu
https://doi.org/10.1016/j.cell.2018.12.041

SUMMARY

Sexually naive animals have to distinguish between the sexes because they show species-typical interactions with males and females without meaningful prior experience. However, central neural pathways in naive mammals that recognize sex of other individuals remain poorly characterized. We examined the role of the principal component of the bed nucleus of stria terminalis (BNSTpr), a limbic center, in social interactions in mice. We find that activity of aromatase-expressing BNSTpr (AB) neurons appears to encode sex of other animals and subsequent displays of mating in sexually naive males. Silencing these neurons in males eliminates preference for female pheromones and abrogates mating success, whereas activating them even transiently promotes male-male mating. Surprisingly, female AB neurons do not appear to control sex recognition, mating, or maternal aggression. In summary, AB neurons represent sex of other animals and govern ensuing social behaviors in sexually naive males.

INTRODUCTION

Sexually reproducing animals display sex differences in social behaviors that enhance reproductive success. Many sexually dimorphic behaviors are acquired traits, but others, such as mating or aggression, are innate in that they can be displayed without prior experience. Such primal interactions are guided by the sex of interacting individuals, indicating that naive animals recognize the sex of their conspecifics. Indeed, naive male mice mate with females but attack males. Neurons in the medial amygdala (MeA) and ventrolateral part of ventromedial hypothalamus (VMHvl) govern these behaviors in male mice (Hong et al., 2014; Lee et al., 2014; Unger et al., 2015; Yang et al., 2013, 2017; Yao et al., 2017), but only reliably code for sex following experience with females (Li et al., 2017; Remedios et al., 2017). Thus, other neurons must recognize the sex of conspecifics in naive mice.

The BNSTpr (also referred to as BNSTmpm) expresses genes in a sexually dimorphic manner, including in humans, and Fos studies implicate it in social behaviors (Gammie and Nelson, 2001; Pfaus and Heeb, 1997; Ramos and DeBold, 2000; Shah et al., 2004; Stack et al., 2002; Wersinger et al., 1997; Wu et al., 2009; Xu et al., 2012; Yang et al., 2013; Zhou et al., 1995). BNSTpr neurons are juxtaposed with other functionally and molecularly heterogeneous BNST subnuclei that can also be sex hormone sensitive, and they are embedded in neural pathways underlying sexually dimorphic behaviors, including the MeA, VMHvl, and preoptic hypothalamus (POA) (Cooke and Simerly, 2005; Crestani et al., 2013; Dong and Swanson, 2004; Giardino et al., 2018; Gu et al., 2003; Guillamón et al., 1988; Moga et al., 1989; Nelson and Trainor, 2007; Segovia and Guillamón, 1993; Simerly, 2002; Swanson, 2000; Walker et al., 2003; Zardetto-Smith et al., 1994). In mice and other animals, BNSTpr neurons are innervated by accessory olfactory bulb (AOB) neurons and are therefore one synapse away from neurons in the vomeronasal organ (VNO) (Broadwell, 1975; von Campenhausen and Mori, 2000; Davis et al., 1978). VNO neurons detect volatile and non-volatile pheromones, chemosensory cues that signal sexual, social, or reproductive status of an animal to other conspecifics (Chamero et al., 2007; Isogai et al., 2011; Kimoto et al., 2005; Liberles, 2014; Trinh and Storm, 2003). Finally, BNST lesions lead to deficits in sexual behavior in male rodents (Claro et al., 1995; Emery and Sachs, 1976; Lehman et al., 1983; Liu et al., 1997; Powers et al., 1987; Valcourt and Sachs, 1979). Despite these advances, the specific functions of BNSTpr neurons in social behaviors remain unclear because of a lack of markers that enable targeted studies of these cells.

Aromatase, which converts androgens to estrogens, is restricted to a subset of BNSTpr neurons in the mouse BNST (Fisher et al., 1998; Lephart, 1996; Naftolin et al., 1971; Wu et al., 2009). Both aromatase and estrogens are essential for development and functioning of sexually dimorphic social behaviors in the two sexes (Arnold, 2009; Honda et al., 1998; Matsumoto et al., 2003; McCarthy, 2008; Toda et al., 2001; Yang and Shah, 2014). We used genetically engineered mice to test the role of AB neurons in sexually dimorphic social behaviors. Calcium imaging of AB neurons in sexually naive males revealed that these cells are differentially activated by males and females. Functional manipulations reveal that these neurons are necessary to distinguish the sexes and for ensuing social interactions, and that their activation elicits male-male mating. By contrast, female AB neurons appear not to participate in sex recognition

Fiber photometry-based imaging of aromatase+ BNSTpr neurons

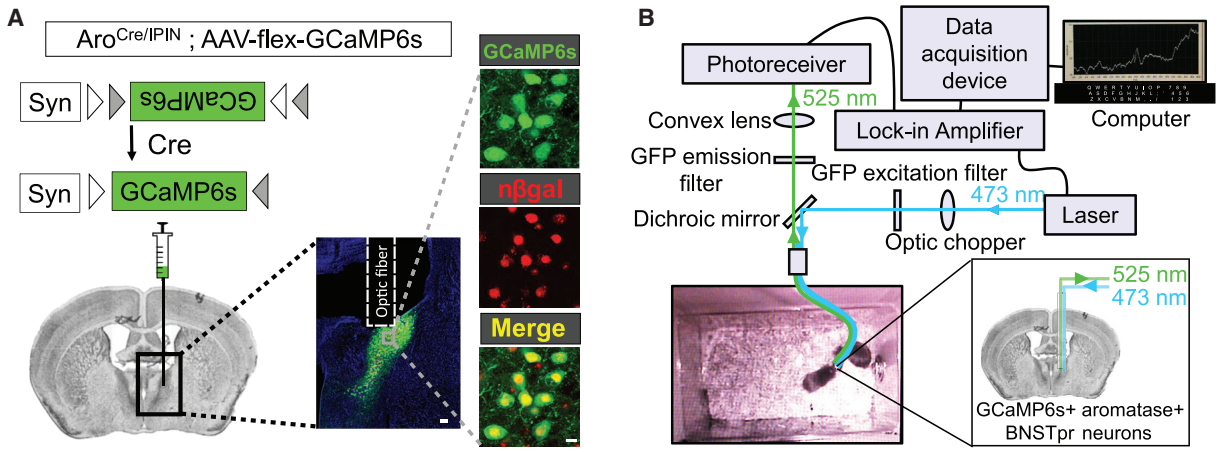

In sexually naive males, neurons respond early, but not during aggression, toward male intruders

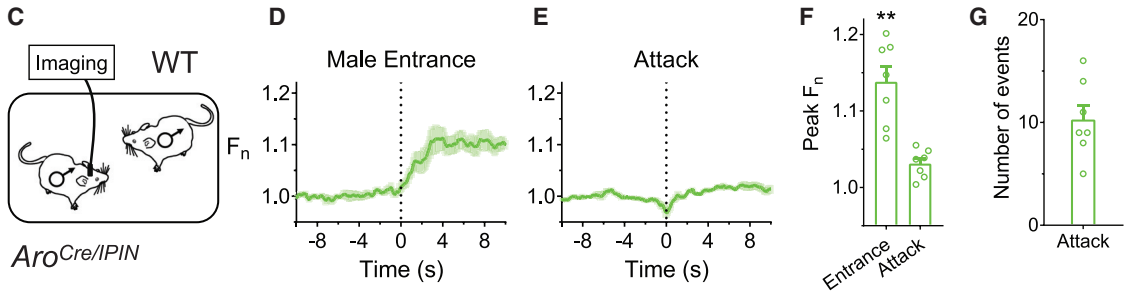

In mothers, neurons respond early, but not during aggression, toward male intruders

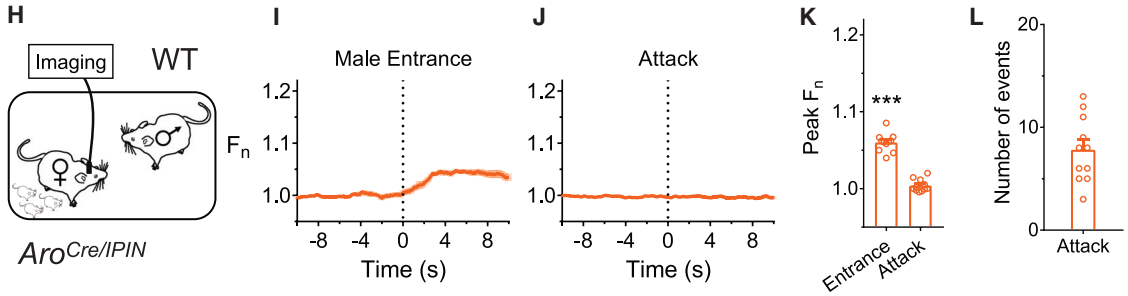

In mothers, neurons respond early, but not during aggression, toward female intruders

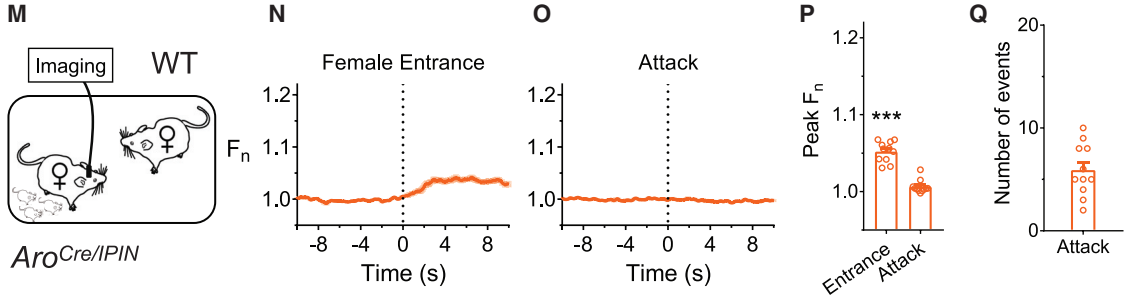

(legend on next page)

or social interactions. Together, AB neurons represent a central neural locus for sex recognition in sexually naive males to direct innate sex specific social behaviors.

RESULTS

AB Neurons Are Active Transiently in Aggressive Encounters

To image activity of AB neurons, we expressed a virally encoded Cre-dependent calcium sensor GCaMP6s in AB neurons in $Aro^{Cre/IPIN}$ mice to perform fiber photometry (Chen et al., 2015; Cui et al., 2013; Gunaydin et al., 2014) (Figures 1A, 1B, and S1A–S1C). $Aro^{Cre/IPIN}$ mice harbor *Cre* and *nuclear LacZ* in the 3′UTR of *aromatase* and enable manipulation of aromatase$^+$ cells in behaviorally and physiologically wild-type (WT) mice (Unger et al., 2015; Wu et al., 2009). We confirmed functional expression of GCaMP6s in AB neurons in slices (Figures S1A–S1E). Next, we singly housed sexually naive $Aro^{Cre/IPIN}$ males and imaged GCaMP6s fluorescence after inserting a WT male intruder. GCaMP6s signal increased with intruder entry and subsided after initial exploration of the intruder (69.1 ± 11.7 s to return to baseline, mean ± SEM, n = 7) (Figures 1C, 1D, and 1F; Video S1). Following early exploration, resident males sniff (anogenital chemoinvestigation), tail rattle, or attack the intruder (Scott, 1966; Unger et al., 2015). We did not detect changes in GCaMP6s signal during these behaviors (Figures 1E–1G and S1F–S1H; Video S1) (peak Fn during tail rattles: 1.01 ± 0.002, p = 0.34, n = 7). GCaMP6s lacks high temporal resolution, and it is possible that baseline firing of AB neurons is higher during an encounter with an intruder than single housing. Nevertheless, baseline fluorescence (p = 0.41, n = 7) was comparable between these two settings. A recent study reported that sexually naive resident males do not attack intruder males (Remedios et al., 2017). By contrast, sexually naive $Aro^{Cre/IPIN}$ resident males clearly attack intruder males, consistent with prior work and our tests with WT males (Figures 1G and S1I–S1N) (Connor, 1972; Crawley et al., 1975; King, 1957; Leypold et al., 2002; Maruniak et al., 1986; Stowers et al., 2002; Takahashi and Miczek, 2014; Yang et al., 2017). Technical differences in this recent study (Remedios et al., 2017) may have altered WT male behavior. Together, our findings show that sexually naive males attack males, and male AB neurons are active early in an encounter with males but not during attacks.

Females do not attack adults unless they are nursing (Gandelman, 1972), when they display maternal aggression and attack intruders. We therefore imaged GCaMP6s fluorescence in AB neurons of $Aro^{Cre/IPIN}$ mothers (Figure S1O). Although females have ~30% fewer AB neurons than males (Wu et al., 2009), we easily detected increased activity of female AB neurons upon insertion of intruders of either sex (Figures 1H–1Q; Video S1). Similar to resident males (Figures 1E and 1F), GCaMP6s signal did not change when mothers attacked or sniffed intruders (Figures 1J, 1K, 1O, 1P, and S1P–S1U; Video S1) or even when they retrieved their pups (Figures S1V–S1A′). In summary, AB neurons are active early in an agonistic encounter in resident males and mothers but not during attacks.

Mating Activates Male AB Neurons

We imaged AB neurons in singly housed sexually naive $Aro^{Cre/IPIN}$ males during mating with a WT sexually receptive female (Figures 2A and S2A). GCaMP6s signal increased upon entry of the female and subsided to baseline after initial exploration (97.7 ± 10.5 s, n = 7) (Figures 2B and 2F; Video S2). Following early exploration, males display bouts of sniffing, mounting, and intromission (penetration) that can result in ejaculation (Figures 2G and S2D). AB neurons responded to mounts, intromission, and ejaculation, but not sniffing (Figures 2C–2F, S2B, and S2C; Video S2), indicating that they are active in many but not all interactions with females.

We also imaged AB neurons in singly housed, sexually naive, receptive $Aro^{Cre/IPIN}$ females that were inserted into a WT male's cage (Figure S2E). Surprisingly, these cells were not activated during these interactions (Figures 2H–2N and S2F–S2K; Video S2). These cells also did not respond appreciably during interactions with a WT receptive female that was inserted into their cage (Figures S2L–S2N). Female BNSTpr neurons are thought to be

Figure 1. AB Neurons Are Transiently Activated in Aggressive Encounters

(A) Strategy to express GCaMP6s in AB neurons. Coronal section through adult male BNST (middle) expressing GCaMP6s and nuclear β-galactosidase (scale bar, 100 μm). Midline is on right, and tract of optic fiber implant is outlined dorsal to BNST. Insets show higher magnification of gray box in the middle panel (scale bar, 10 μm).

(B) Fiber photometry setup to image GCaMP6s in a freely behaving mouse.

(C–Q) Fiber photometry imaging of AB neurons in singly housed $Aro^{Cre/IPIN}$ male (C–G) or mother (H–Q) interacting with WT intruder for 15 min.

(C) A WT male is inserted into the cage of a sexually naive male.

(D and E) Peri-event time plot (PETP) of GCaMP6s signal around entry of male (D) and onset of attack episodes (E). For PETPs shown in this and other figures, dark colored line and paler shaded region represent mean fluorescence and SEM, respectively. Vertical dashed black line indicates beginning of event or behavior; Fn on y axis of PETP represents fold change from baseline preceding the event.

(F) GCaMP6s signal increases upon entry of male. Peak Fn represents maximal fold change from baseline preceding the event. Tests of significance were performed, unless otherwise mentioned, by comparing peak Fn of various events to baseline GCaMP6s fluorescence preceding the event and correcting for multiple comparisons. (G) Number of attacks by resident male.

(H) Male is inserted into the cage of a mother.

(I–K) GCaMP6s signal increases in mothers upon entry of male (I) but not when she attacks him (J). Data shown as PETP (I and J) and Peak Fn changes (K).

(L) Number of attacks by mothers.

(M) Female is inserted into the cage of a mother.

(N–P) GCaMP6s signal increases in mothers upon entry of female (N) but not when she attacks her (O). Data shown as PETP (N and O) and Peak Fn changes (P).

(Q) Number of attacks by mothers.

Mean ± SEM; hollow circles represent individual mice in these and subsequent figures. n = 7 (C–G), 11 (H–Q). **p < 0.01, ***p < 0.001.

See also Figure S1, Table S1, and Video S1.

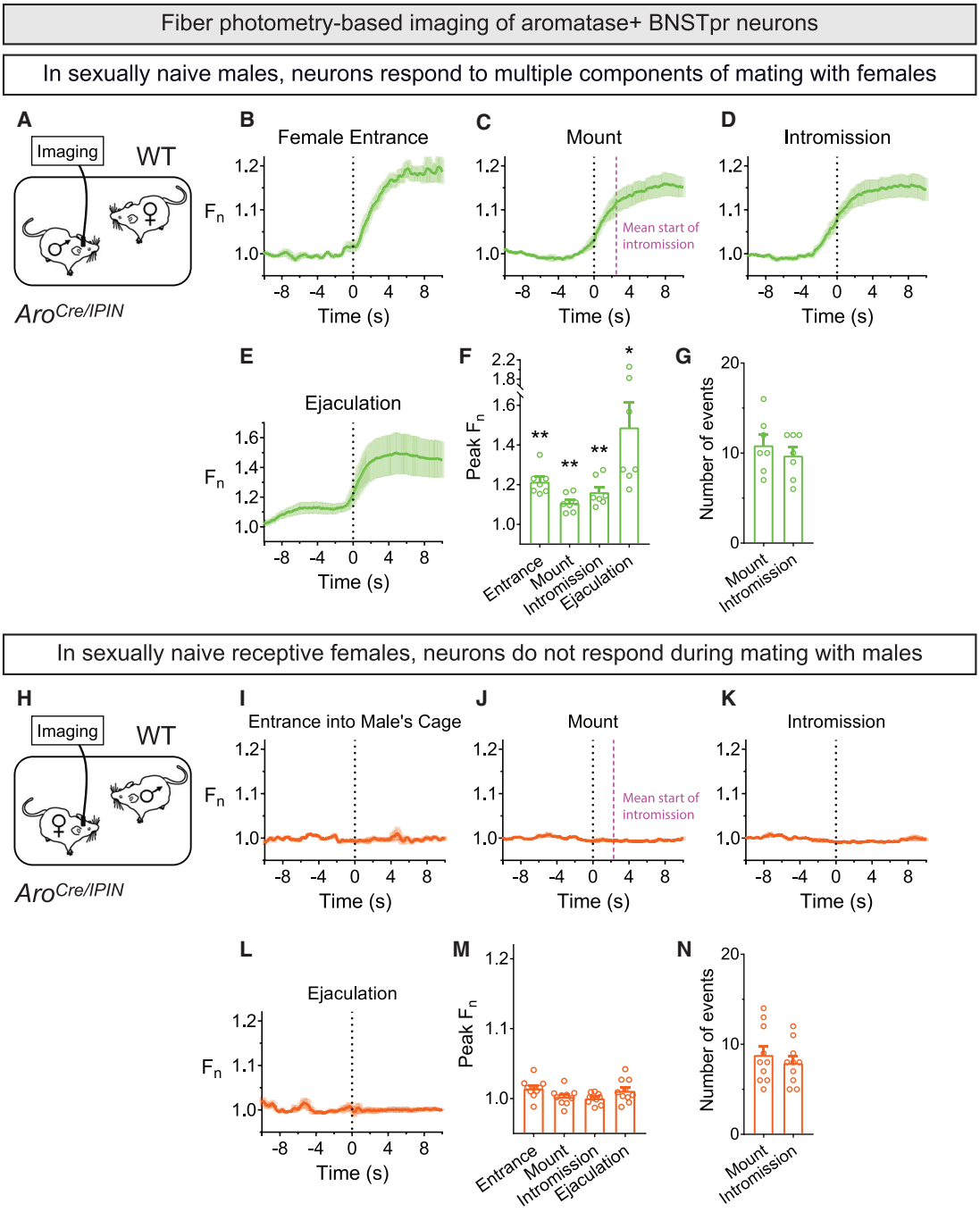

Figure 2. Male AB Neurons Are Active during Interactions with Females

Fiber photometry imaging of AB neurons in sexually naive *Aro*$^{Cre/IPIN}$ males (A–G) or females (H–N) during 30 min test of mating behavior.

(A) Female is inserted into cage of a singly housed male.

(B–F) GCaMP6s signal increases upon entry of female (B), mounting (C), intromission (D), and ejaculation (E). Data shown as PETP (B–E) and Peak Fn changes (F). Dashed pink line in (C) shows mean time at which mounting proceeded to intromission.

(G) Number of mount and intromission events displayed by each male.

(H) A receptive female is inserted into the cage of a WT male.

(I–M) No change in GCaMP6s signal following entry into the male's cage (I), mounting (J), intromission (K), and ejaculation (L). Data shown as PETP (I–L) and Peak Fn changes (M).

(**N**) Number of mounts and intromissions by WT males toward *Aro*$^{Cre/IPIN}$ females.

Mean ± SEM; n = 7 (A–G), 10 (H–N). *p < 0.05, **p < 0.01.

See also Figure S2, Table S1, and Video S2.

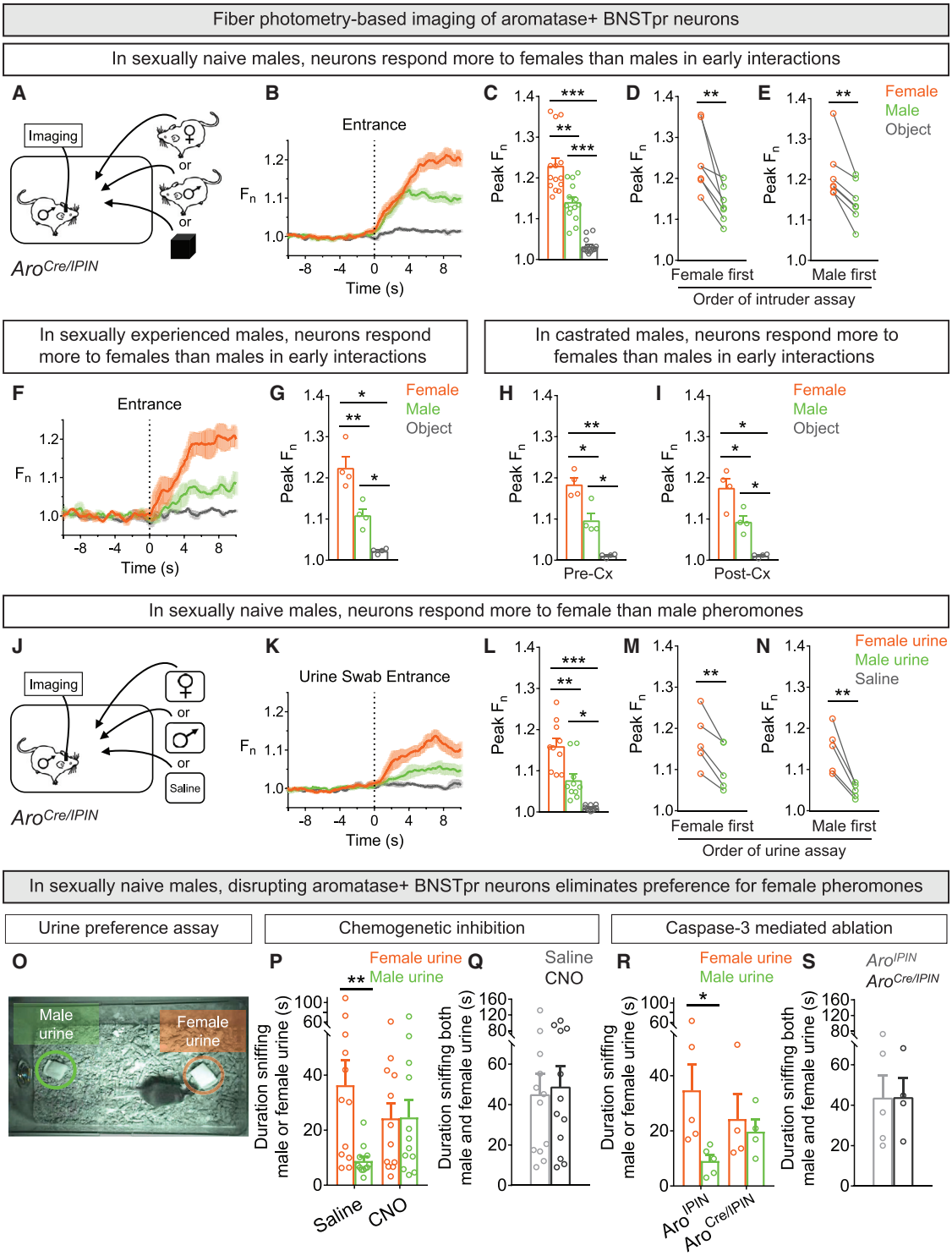

Figure 3. Male AB Neurons Respond Differently to the Two Sexes and Regulate Sexual Preference

(A–N) Fiber photometry of AB neurons in singly housed *Aro*$^{Cre/IPIN}$ male.

(A–I) A WT male, receptive female, or novel object was inserted for 3 min into the cage of a sexually naive male. Experiment schematized in (A).

(B and C) Larger change in activity of AB neurons upon entry of female compared to male. Males or females elicited larger response compared to object. Data shown as PETP (B) and Peak Fn changes (C).

(D and E) AB neurons responded more to a female irrespective of whether they were exposed first to a female (D) or male (E).

(legend continued on next page)

active during mating (Pfaus and Heeb, 1997). AB neurons are a subset of the BNSTpr (Wu et al., 2009), suggesting that, in females, aromatase$^-$ BNSTpr neurons are active during mating. We do not have a mouse line to image just the entire BNSTpr or aromatase$^-$ BNSTpr neurons. Most BNSTpr neurons and neighboring BNST subnuclei are GABAergic (Figures S2O–S2S) (Ng et al., 2009). We therefore imaged GABAergic BNST neurons in receptive *Vgat*^{Cre} females (Vong et al., 2011) mating with WT males and found that these cells were activated during these interactions (Figures S2T–S2X; Video S2). Thus, we can detect activation of AB neurons in receptive females, thereby excluding technical issues with fiber photometry in this context. Although sexual experience increases female receptivity (Thompson and Edwards, 1971; Xu et al., 2012), Vgat$^+$ BNST neurons were active during mating in sexually naive females. Thus, lack of sexual experience is unlikely to underlie the lack of detectable activity in AB neurons during mating. In summary, AB neurons are active during male but not female mating behavior.

Activity of AB Neurons in Sexually Naive Males Distinguishes between the Sexes

The activity of male AB neurons appeared larger upon entry of a female than a male intruder (Figures 1D and 2B). To test this directly in individual males, we imaged AB neurons in singly housed, sexually naive *Aro*$^{Cre/IPIN}$ males with intruders of both sexes (Figures 3A and S3A). AB neurons were specifically activated more upon entry of a female than a male regardless of the order of entry of intruders (Figures 3B–3E). This sex-typical response reflects neither absolute differences in early interactions with the two sexes (Figures S3B and S3C) nor experience in mating or fighting because these behaviors were not observed in this brief 3 min test. Whether the same subset of AB neurons responds to the two sexes will entail probing these cells with single cell RNA sequencing (RNA-seq) combined with functional studies. Importantly, AB neurons in sexually experienced males also responded more to females than males (Figures 3F, 3G, and S3E), indicating that mating does not alter AB neuronal responses to the two sexes.

These results suggest that male AB neurons encode or relay information relating to sex of conspecifics. Alternatively, they might encode motor drive or motivation to mate or fight. To distinguish between these models, we imaged AB neurons of sexually naive resident males during 3 min encounters with male or female intruders before and after castrating (Cx) the residents (Figures 3H, 3I, S3F, and S3G). AB neuron responses were comparable between pre-Cx and Cx males (Figures 3H and 3I). Cx males did not mate (0/4) with WT receptive females in 30 min assays, confirming functional absence of testosterone. Thus, male AB neurons respond differentially to the two sexes even when males do not mate or fight, indicating that the sex-typical response of these cells corresponds to sex recognition rather than purely motivational states or motor drives for social behaviors.

Mice use pheromones to distinguish the sexes (Baum and Bakker, 2013; Leypold et al., 2002; Stowers et al., 2002), suggesting that the early sex-typical response of AB neurons was elicited by intruder pheromones. We tested whether urine, a source of pheromones that can signal conspecific sex (Fu et al., 2015; Haga-Yamanaka et al., 2014; He et al., 2008; Holy et al., 2000; Kimoto et al., 2007; Meeks et al., 2010; Nodari et al., 2008; Tolokh et al., 2013), activated AB neurons. We imaged AB cells of sexually naive *Aro*$^{Cre/IPIN}$ males after inserting cotton swabs wetted with male or female urine or saline (Figures 3J and S3D). AB neurons responded more to urine than to saline and more to female than male urine (Figures 3K–3N; Video S3). This response was smaller compared to insertion of mice (Figures 3A–3C), suggesting that other cues also activate AB neurons. Unlike AB neurons, VNO neurons can respond in a binary manner to male or female urine (Holy et al., 2000). AOB mitral neurons, which are postsynaptic to VNO neurons, also show complex responses to the two sexes (Luo et al., 2003), suggesting significant transformation of sex recognition signals downstream of the VNO. Importantly, AB neurons did not respond to 2-phenylethylamine (PEA) or cadaverine, cues found in predator urine and decomposing tissue respectively (Ferrero et al., 2011; Liberles, 2014, 2015) (Figures S3H–S3J). Thus, AB neurons respond selectively and differentially to pheromones from male and female conspecifics.

Male mice prefer sniffing female to male urine (Baum and Bakker, 2013; Mandiyan et al., 2005; Pankevich et al., 2004; Yao et al., 2017), and we tested if disrupting AB neurons would alter this preference (Figure 3O). We silenced AB neurons of sexually naive males with an inhibitory DREADD (DREADDi) and found

(F and G) Larger change in activity of AB neurons upon entry of female compared to male. Males and females elicited larger response compared to object. Data shown as PETP (F) and Peak Fn changes (G).
(H and I) Larger change in activity of AB neurons in sexually naive males prior to (H) and after (I) Cx upon entry of female compared to male. Males and females elicited larger response compared to object.
(J–N) A cotton swab wetted with female or male urine or saline was inserted for 3 min each into cage of a *Aro*$^{Cre/IPIN}$ male. Experiment schematized in (J).
(K and L) AB neurons responded more to swab wetted with female compared to male urine. Urine wetted swabs elicited larger response compared to saline. Data shown as PETP (K) and Peak Fn changes (L).
(M and N) Female urine elicited larger response irrespective of whether the male was exposed first to female (M) or male (N) urine.
(O–S) Cotton swabs wetted with male or female urine were simultaneously inserted into the cage of *Aro*$^{Cre/IPIN}$ males expressing DREADDi (O, P, and Q) or engineered caspase-3 (O, R, and S) to enable inhibition or ablation of AB neurons. *Aro*^{IPIN} males injected with caspase-3 payload served as controls (R and S).
(P) CNO eliminates preference for female urine.
(Q) Males given saline or CNO sniffed both swabs for similar total duration.
(R) Ablation of AB neurons eliminates preference for female urine.
(S) Both groups of males sniffed both swabs for similar total duration.
Mean ± SEM; n = 14 (A–E), 4 (F–I), 10 (J–N), 12 (P and Q), 5 (R and S, *Aro*^{IPIN}), 4 (R and S, *Aro*$^{Cre/IPIN}$). *p < 0.05, **p < 0.01, ***p < 0.001.
See also Figure S3, Table S1, and Video S3.

that this abolished preference for female urine (Sternson and Roth, 2014) (Figures 3P and S3K–S3Q). The total time spent sniffing urine was unaltered (Figure 3Q), indicating that inhibiting AB cells does not disrupt the drive to chemoinvestigate objects. Acute manipulation of neuronal activity can disrupt systemic network function (Südhof, 2015), so we disrupted AB neurons with a complementary approach. We expressed in male AB neurons a designer caspase that leads to Cre-dependent autonomous apoptosis (Morgan et al., 2014; Yang et al., 2013) and found that ablation of AB cells also abolished preference for female urine (Figures 3R, 3S, S3R, and S3S). In contrast to our photometry findings in males, AB neurons in mothers responded similarly to male and female intruders or insertion of male or female urine wetted swabs (Figures S3T–S3C′). In summary, male AB neurons provide information about intruder sex and regulate innate preference for female pheromones.

Male AB Neurons Require Vomeronasal Pheromone Sensing to Distinguish between the Sexes

Male and female pheromones are sensed by distinct VNO neurons and AOB mitral cells (Ben-Shaul et al., 2010; Hammen et al., 2014; Holy, 2018; Luo et al., 2003). AOB mitral cells project to the BNSTpr (Broadwell, 1975; von Campenhausen and Mori, 2000; Davis et al., 1978), suggesting that this pathway drives the pheromone-elicited response of AB neurons. Indeed, Fos studies suggest a role for the VNO in activating BNSTpr (Halem et al., 1999; Pankevich et al., 2006). We first tested whether VNO pheromone sensing guided male preference for female urine. The cation channel Trpc2 is critical for VNO pheromone transduction, and *Trpc2*$^{-/-}$ males do not distinguish between the sexes (Leypold et al., 2002; Stowers et al., 2002). Although Trpc2 is expressed in some main olfactory epithelium (MOE) neurons, it's function in MOE neurons is unclear (Omura and Mombaerts, 2014). In any event, *Trpc2*$^{-/-}$ males did not show a preference for female urine (Figures 4A–4C). We next imaged AB neurons in sexually naive *Aro*$^{Cre/IPIN}$;*Trpc2*$^{-/-}$ males and found that they responded similarly to urine from both sexes (Figures 4D–4G and S4A). They also responded specifically and similarly to entry of a female or male intruder in a 3 min assay that precluded mating or aggression (Figures 4H–4K). Activity of AB neurons upon presentation of female urine or intruder was comparable between *Aro*$^{Cre/IPIN}$ and *Aro*$^{Cre/IPIN}$;*Trpc2*$^{-/-}$ males (peak Fn for female urine: *Aro*$^{Cre/IPIN}$ = 1.16 ± 0.02, n = 10, and *Aro*$^{Cre/IPIN}$;*Trpc2*$^{-/-}$ = 1.18 ± 0.02, n = 5, p = 0.44; peak Fn for female intruder: *Aro*$^{Cre/IPIN}$ = 1.23 ± 0.02, n = 14, and *Aro*$^{Cre/IPIN}$;*Trpc2*$^{-/-}$ = 1.24 ± 0.03, n = 5, p = 0.77) (Figures 3C, 3L, 4F, and 4J). By contrast, their activity was larger upon presentation of male urine or intruder in *Aro*$^{Cre/IPIN}$;*Trpc2*$^{-/-}$ males than *Aro*$^{Cre/IPIN}$ males (peak Fn for male urine: *Aro*$^{Cre/IPIN}$ = 1.08 ± 0.02, n = 10, and *Aro*$^{Cre/IPIN}$;*Trpc2*$^{-/-}$ = 1.18 ± 0.02, n = 5, p = 0.0015; peak Fn for male intruder: *Aro*$^{Cre/IPIN}$ = 1.14 ± 0.01, n = 14, and *Aro*$^{Cre/IPIN}$;*Trpc2*$^{-/-}$ = 1.26 ± 0.03, n = 5, p = 0.0003) (Figures 3C, 3L, 4F, and 4J). Although it is difficult to compare GCaMP6s signal across different animal cohorts, our findings indicate that loss of Trpc2 function increases the response of AB neurons to male pheromones. VNO neurons can detect volatile cues, but at least some of the response of AB neurons to volatile cues likely reflects input from pathways that relay MOE-initiated pheromonal signaling (Brennan et al., 1999; Kang et al., 2009, 2011a, 2011b; O'Connell and Meredith, 1984; Sam et al., 2001; Trinh and Storm, 2003).

VNO and mitral neurons are excitatory, but Trpc2-dependent signaling decreases response of male AB neurons to male pheromones. This may reflect developmental differences in Trpc2 mutants. Alternatively, pheromones excite or inhibit different AOB mitral cells *in vivo* (Luo et al., 2003), and disinhibition of these cells in Trpc2 mutants may elevate the response of AB neurons to male pheromones. The inhibitory influence of Trpc2-dependent signaling on AB neurons could also arise from network interactions locally or elsewhere. In any event, the differential response of male AB neurons to males and females relies on Trpc2-dependent pheromone transduction.

Trpc2$^{-/-}$ males mate with both sexes, and in longer assays (30 min), male AB neurons of *Aro*$^{Cre/IPIN}$;*Trpc2*$^{-/-}$ males were active during mating with either sex (Figures S4B–S4M; Video S4). Males do not intromit or ejaculate when mating with males (Figure S4M), and the activity of AB neurons declined following a mount with a male (Figures S4D–S4H and S4K–S4M). However, peak GCaMP6s signal was comparable during mounts with either sex (peak Fn during mount: with female = 1.31 ± 0.03, and with male = 1.26 ± 0.02, n = 5, p = 0.3359; Figures S4D, S4G, S4K, and S4L). Thus, male AB neurons likely encode or relay information about the sex of conspecifics and regulate preference for female urine in a VNO-dependent manner.

AB Neurons Regulate Male Sexual Behavior

Male AB neurons are active during mating so we tested whether they were required for this behavior. Chemogenetic inhibition of AB neurons of sexually naive males profoundly reduced mating with a WT receptive female (Figures 5A–5C and S5A). Most males did not mount or intromit, and none ejaculated, demonstrating a role of AB neurons in mating success. We did not find pervasive deficits in behavior (Figures 5B, 5C, and S5B–S5G) or aggressive displays (0/14 males attacked females). These deficits were also observed in sexually naive males in whom we ablated AB neurons (Figures 5D–5F and S5H–S5L). These males, in fact, mounted less and did not intromit (Figures 5E and 5F), suggesting that DREADDi inhibition may have incompletely eliminated AB neuronal function. Female AB neurons are not active during sexual behavior (Figures 2H–2N and S2I–S2K), and inhibition or ablation of these cells in *Aro*$^{Cre/IPIN}$ females did not alter receptivity or other behaviors (Figures 5G–5N and S5M–S5W). In summary, AB neurons are required, both acutely and chronically, for WT levels of male mating.

AB Neurons Regulate Male Aggression

We next tested the males previously assayed with females (Figures 5A–5F) with a WT male intruder. Both chemogenetic inhibition and ablation of AB neurons lowered the probability and reduced number of attacks without triggering mating (Figures 6A–6F, S5E, S6A, and S6B). These findings suggest that the early response of AB neurons to males is critical for aggression. More generally, the diminution in aggression and mating following disruption of male AB neurons suggests that inability

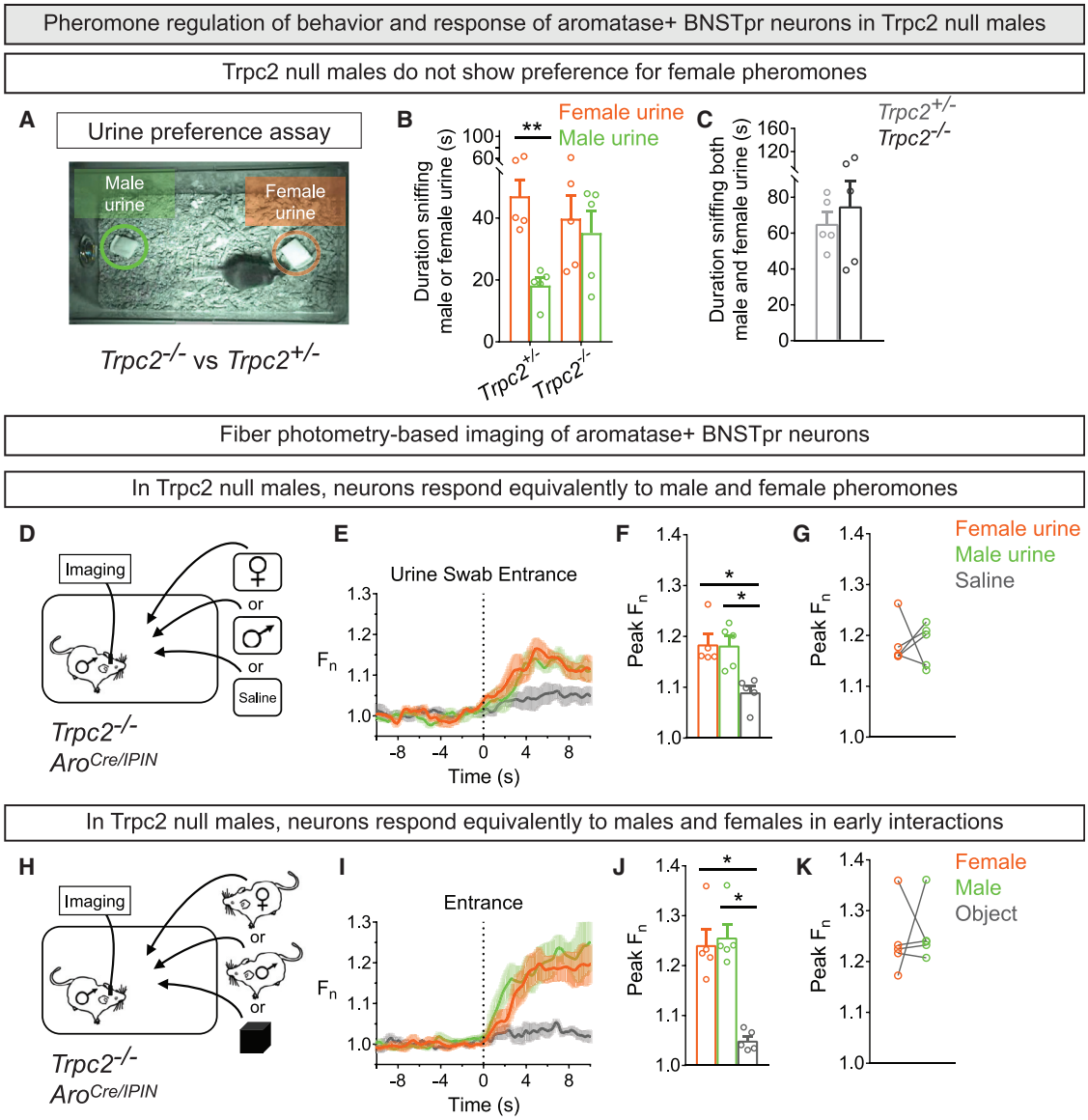

Figure 4. Sex-Typical Response of Male AB Neurons Is Dependent on Pheromone Sensing

(A–C) Sexually naive *Trpc2*$^{-/-}$ and *Trpc2*$^{+/-}$ males were tested for urine preference. Experiment schematized in (A).

(B) *Trpc2*$^{-/-}$ males sniff male and female urine equally.

(C) *Trpc2*$^{-/-}$ and *Trpc2*$^{+/-}$ males sniff male and female urine for similar total duration.

(D–K) Fiber photometry of AB neurons in singly housed males exposed to urine swab (D–G) or male, female, or novel object inserted into the cage for 3 min (H–K).

(D) A cotton swab wetted with female or male urine or saline was inserted into the cage.

(E and F) Response of AB neurons was similar to male or female urine and larger than that to saline. Data shown as PETP (E) and Peak Fn changes (F).

(G) Similar response to male or female urine.

(H) A WT male, receptive female, or novel object was inserted into the cage.

(I and J) Response of AB neurons was similar to male or female intruder and larger than that to the object. Data shown as PETP (I) and Peak Fn changes (J).

(K) Similar response to male or female intruder.

Mean ± SEM; n = 5 males/genotype. *p < 0.05, **p < 0.01.

See also Figure S4 and Video S4.

to recognize males and females leads to a loss of meaningful interactions.

We next tested the role of AB neurons in maternal behavior. Neither chemogenetic inhibition nor targeted ablation of these cells led to detectable deficits in pup retrieval, maternal aggression, or other behaviors (Figures 6G–6L and S6C–S6R). Ablation of AB neurons also did not alter litter size or percent pups surviving to weaning (Figures S6N–S6P). We cannot exclude incomplete functional disruption of female AB neurons, but we did observe behavioral deficits with similar manipulations in males.

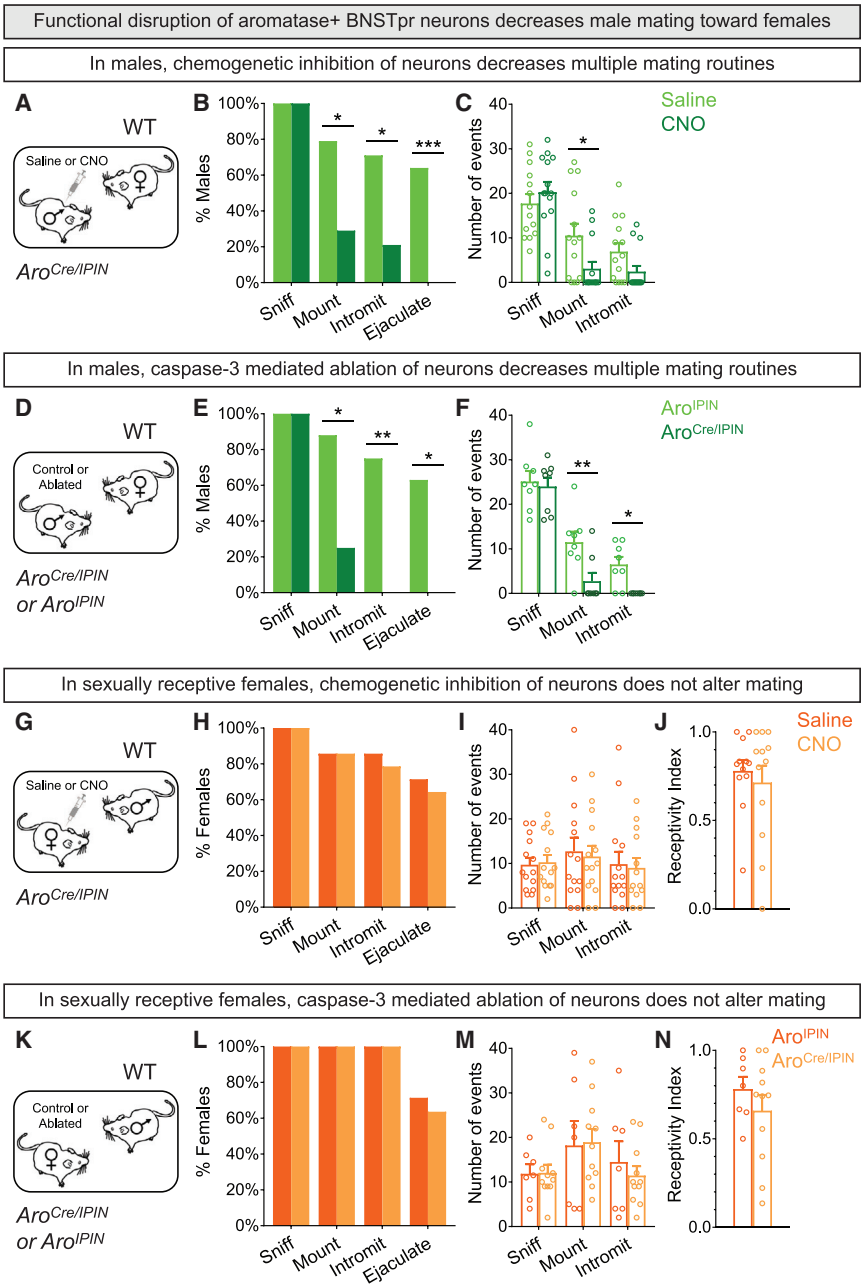

Figure 5. AB Neurons Play an Essential Role in Male Mating

(A–C) Behavior of singly housed male expressing DREADDi in AB neurons with receptive female intruder (A).

(B) CNO reduced percent males mounting or intromitting and eliminated ejaculation.

(C) CNO reduced mounts per assay.

(D–F) Behavior of singly housed males with caspase-3 targeted to AB neurons with receptive female intruder (D).

(E) Ablation of AB neurons reduced percent males mounting and precluded intromission or ejaculation.

(F) Ablation of AB neurons reduced mounts and intromissions per assay.

(G–J) Behavior of receptive female expressing DREADDi in AB neurons upon insertion into male cage (G).

(H–J) Behavior of females given CNO or saline is comparable for percent females showing behavior (H), number of behavioral events (I), and receptivity index (J).

(K–N) Behavior of receptive females with caspase-3 targeted to AB neurons upon insertion into male cage (K).

(L–N) Behavior of both groups of females is comparable for percent females showing behavior (L), number of behavioral events (M), and receptivity index (N).

Mean ± SEM; n = 14 (A–C), 8 (D–F, each genotype), 14 (G–J), 7 (K–N, Aro^{IPIN}), and 11 (K–N, $Aro^{Cre/IPIN}$). *p < 0.05, **p < 0.01, ***p < 0.001.

See also Figure S5 and Table S1.

It is more likely that alternative neural pathways in the amygdala and hypothalamus are important for maternal care (Hashikawa et al., 2017; Unger et al., 2015). Thus, AB neurons appear to contribute minimally to maternal care but are critical for male aggression.

Persistent Activation of Male AB Neurons Promotes Male-Male Mating

We wondered if optogenetic activation of male AB neurons would promote male mating. We expressed channelrhodopsin-2 (ChR2) (Fenno et al., 2011) in AB neurons of sexually naive males and tested their behavior with WT male or receptive female intruders. Strikingly, laser illumination (473 nm, 5 Hz, 5 ms pulse width, 30-s cycles, 2 mW) upon insertion of a male suppressed aggression and elicited mounting (Figures 7A–7D, S7A, S7B, and S7E–S7K; Video S5). The few males (2/8) who attacked the intruder also mounted them. Mating attempts or attacks were not time-locked to laser illumination (Figure S7C), and the latency to initiate mounting toward the male was similar to male mating attempts with a female (mount latency to females and males, respectively, 447.1 ± 82.1 s and 365.3 ± 90.7 s, n = 5 females and 6 males, p = 0.5317; Figure 7D).

Activation of male AB neurons may not have triggered time-locked mating because intruder males are not receptive. However, optogenetic activation did not elicit time-locked mating with WT receptive females with the above (Figure S7D) or a different set of stimulation parameters (20 Hz, 20 ms pulse width, 30-s cycles, 2 mW; n = 3). We also did not detect aberrant sexual behavior with females in that the latency to initiate and the number of various routines were unchanged (Figures 7E–7H).

Optogenetic activation of AB neurons in receptive females did not alter their mating with WT males nor did it elicit male-type

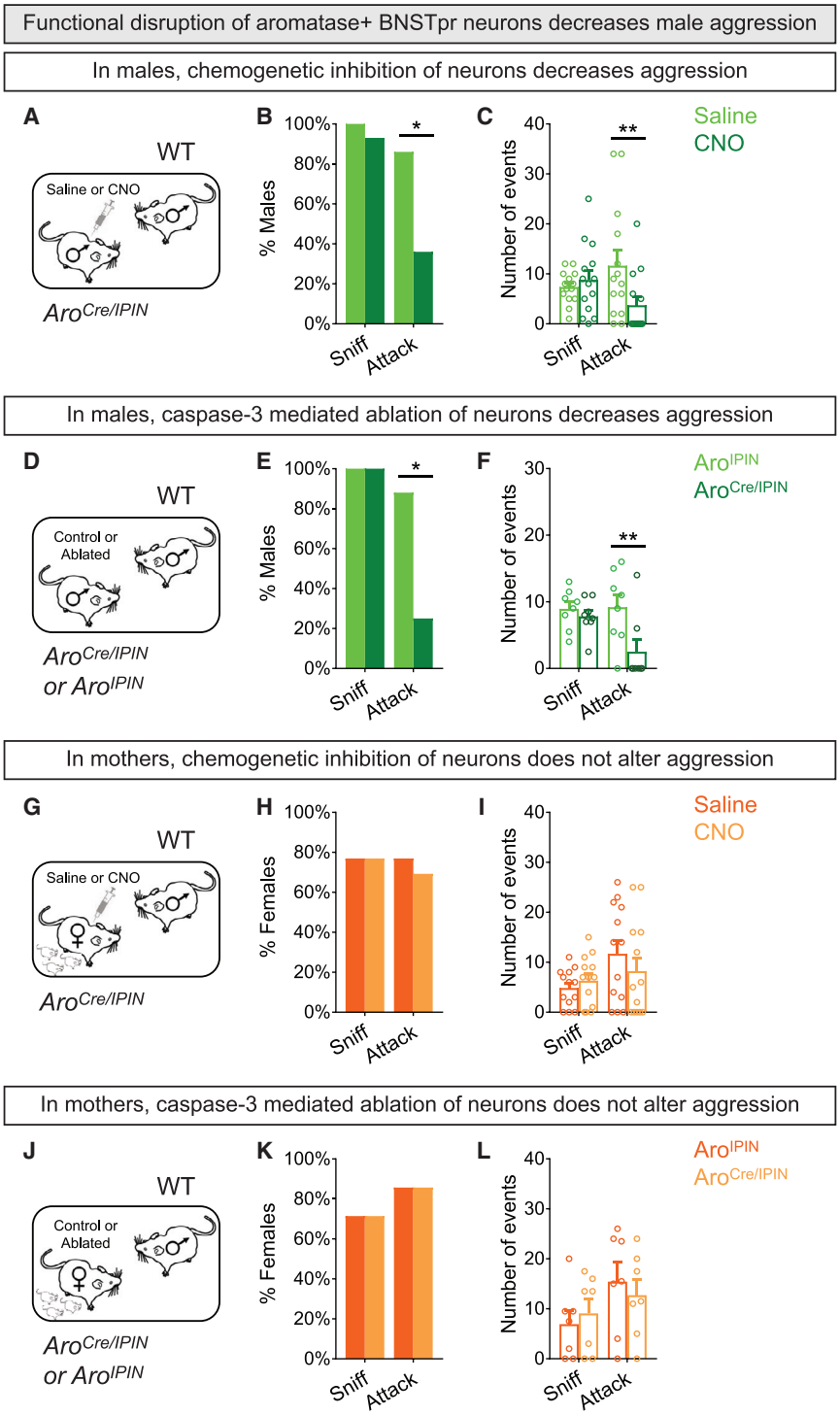

Figure 6. AB Neurons Play an Essential Role in Male Aggression

(A–C) Behavior of resident male expressing DREADDi in AB neurons with WT male intruder (A).
(B) CNO reduced percent residents attacking.
(C) CNO reduced attacks per assay.
(D–F) Behavior of resident males with caspase-3 targeted to AB neurons with WT male intruders (D).
(E) Ablation of AB neurons reduced percent residents attacking.
(F) Ablation of AB neurons reduced attacks per assay.
(G–I) Behavior of mothers expressing DREADDi in AB neurons with male intruder (G).
(H and I) Behavior of mothers given CNO or saline is comparable for percent mothers showing behavior (H) and number of behavioral events (I).
(J–L) Behavior of mothers with caspase-3 targeted to AB neurons with male intruder (J).
(K and L) Behavior of both groups of mothers is comparable for percent mothers showing behavior (K) and number of behavioral events (L).
Mean ± SEM; n = 14 (A–C), 8 (D–F, each genotype), 13 (G–I), 7 (J–L, each genotype). *p < 0.05, **p < 0.01.
See also Figure S6 and Table S1.

mounting (Table S1). Activating AB neurons in mothers also did not elicit male-type mating nor did it impair pup retrieval or aggression toward a male (Table S1). These findings complement the lack of a discernible behavioral phenotype after disrupting female AB neurons. Thus, activating AB neurons in males but not females inhibits aggression and biases the male to initiate mating toward males. In addition, the latency to mate with females is unchanged, indicating that early activation of male AB neurons upon encountering a female (Figures 2B, 2F, 3B, 3C, 3K, and 3L) is salient and cannot be enhanced functionally by optogenetic activation.

Early Activity of Male AB Neurons Promotes Mating

To test the relevance of early activity of male AB neurons, we used halorhodopsin (eNpHR3.0) to inhibit it in sexually naive males (Fenno et al., 2011) (Figure S7L). We switched the laser on (593.5 nm, 6 mW), immediately inserted a WT receptive female, and then switched the laser off after 90 s, well before any mating attempts (0/8 males mounted a female in first 90 s) (Figure 7I). This brief inhibition delayed the onset of mating 3-fold, reduced mounting, increased latency to intromit and ejaculate (Figure 7J-L), and did not elicit aggression (0/8 males attacked females). Similar to DREADDi inhibition and ablation studies, optogenetic inhibition for the entire test profoundly reduced male mating (Figures 5A–5F and S7M–S7O). That males eventually mated after early transient inhibition suggests that they could subsequently process female cues that elicit this behavior. Together, these studies show that early activity of male AB neurons is critical for mating.

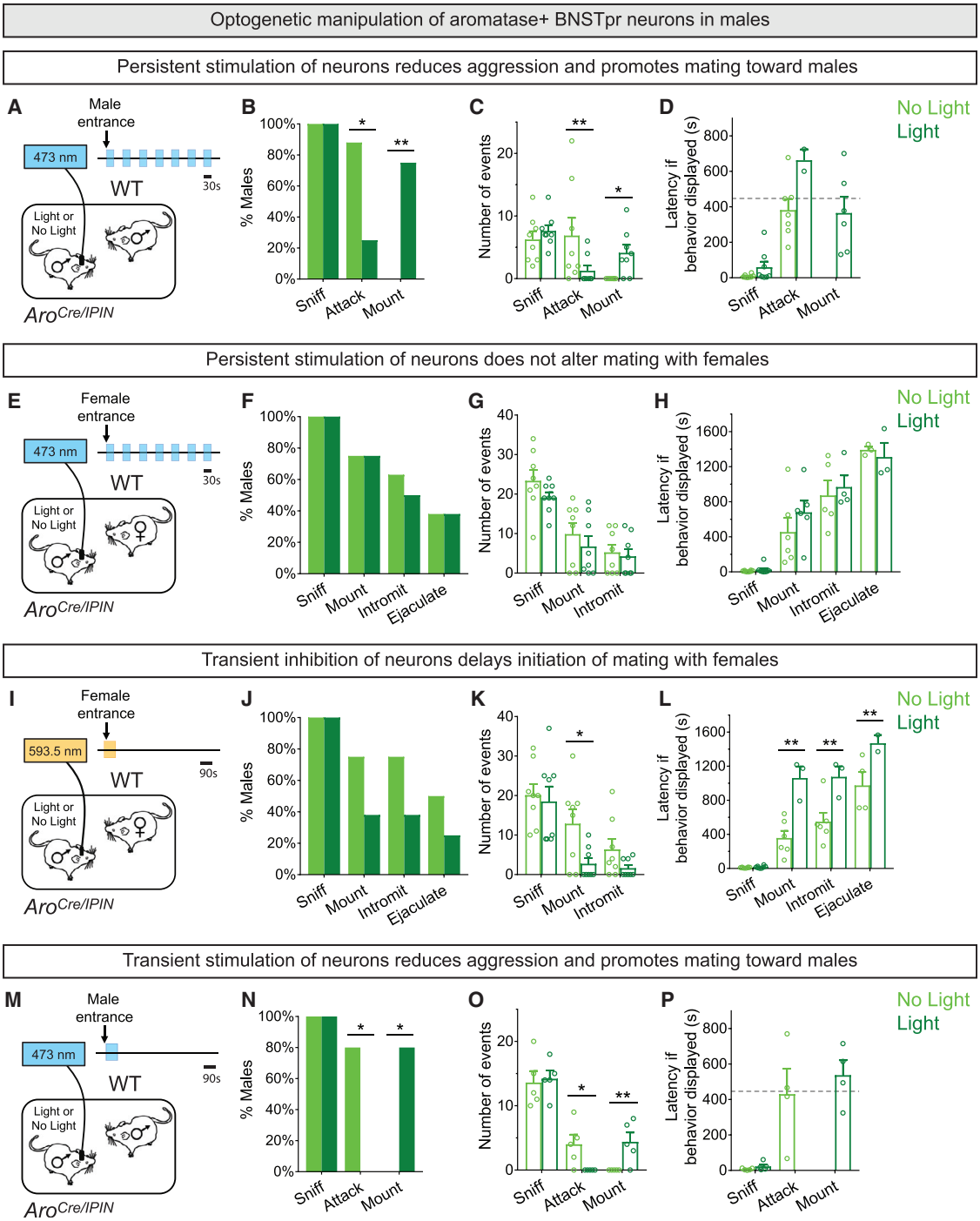

Figure 7. Early Activity in Male AB Neurons Promotes Mating and Inhibits Fighting

(A–D) Laser illumination of ChR2+ AB neurons in resident males interacting with WT intruder male for 15 min (A).

(B) Laser illumination reduces probability of attacks and increases that of mounts toward the intruder.

(C) Laser illumination reduces attacks and increases mounts toward the intruder per assay.

(D) Latency to mount male intruder is similar to latency to mount receptive female intruder (shown by horizontal dashed line). Data for males mating with females is from (H).

(E–H) Laser illumination of ChR2^{+} AB neurons in resident males interacting with receptive female intruder for 30 min (E).

(F–H) Laser illumination does not alter mating with females as assayed by percent males showing behavior (F), number of behavioral events (G), and latency to initiate behavior (H).

(I–L) Brief (90 s) laser illumination of eNpHR3.0^{+} AB neurons in resident males interacting with receptive female intruders for 30 min (I).

(legend continued on next page)

We next tested whether reducing laser power would elicit aggression toward receptive female intruders in a subset of these $Aro^{Cre/IPIN}$ males (5 mW, 3 mW, 1 mW; n = 3). Although more males mated with diminishing laser power (0/3, 1/3, 3/3 males mated at 5 mW, 3 mW, and 1 mW, respectively), they never attacked females. This suggests that optogenetic parameters may need to be optimized further or that other pathways inhibit male aggression toward females. In summary, transient early inhibition of male AB neurons delays mating well beyond the duration of laser illumination, demonstrating an enduring influence of the early activity of AB neurons in mating.

Male AB neurons also respond early in intermale encounters, but this response is ~60% lower than the response to females (Figure 3C). We tested if enhancing this early activity would alter ensuing behavior with a male. We inserted a WT male and immediately activated $ChR2^+$ AB neurons of the male residents for 90 s (473 nm, 5 Hz, 5 ms pulse width, 2 mW) (Figures 7M and S7P), a period during which residents did not mate or fight (0/5 residents mated or fought). Strikingly, residents now attempted to mate with rather than attack male intruders (Figures 7N–7P; Video S5). This brief activation did not alter latency to sniff intruders, and the latency to initiate mating was similar to that observed when males mated with females (Figure 7P). We observed mount attempts even toward the end of the 15 min assay, demonstrating a perduring influence of the initial 90 s of stimulation. It is unclear if these enduring behavioral changes reflect alterations in sex recognition or other internal states. Regardless, early activation of male AB neurons seems to provide a signal that induces a long-lasting change such that males functionally misidentify other males as females in the sense that they attempt to mate with them.

DISCUSSION

Naive animals must innately distinguish between the sexes in order to engage in courtship or territorial displays. Neurons that reliably distinguish between males and females in sexually naive mammals have remained elusive, and displays of innate behaviors such as aggression have even been proposed to require sexual experience (Remedios et al., 2017). Here, we show that the activity of AB neurons distinguishes between the sexes in sexually naive males. Together, our findings suggest that these cells are central to deciding the course of action during social encounters. Activity of AB neurons enables a male to distinguish between the sexes and enact a decision to mate with females and attack males. In this model, functional removal of AB neurons precludes males from recognizing the sex of other animals, and virtually eliminates selection of either course of action, mating with females or attacking males.

Role of Male AB Neurons in Social Behaviors

The early response of male AB neurons that distinguishes the sex of intruders relies on Trpc2-dependent signaling, which is also critical to distinguish between the sexes (Leypold et al., 2002; Stowers et al., 2002). These neurons are unlikely to exclusively control motor drive or motivation to mate or fight because disrupting their function does not eliminate motivated behaviors, activating them does not elicit time-locked behavior, and they respond differentially to the two sexes in Cx males who do not mate or fight. Together, our findings suggest that male AB neurons encode Trpc2-dependent information about the sex of conspecifics that is critical for ensuing social behaviors.

Although male AB neurons are active during mating, experimental activation of these cells biases males to mate without eliciting discernible time-locked mating routines. Further optimization of stimulation parameters might elicit time-locked behaviors. Alternatively, activity of AB neurons during mating could reflect sensory input, internal states relating to mating, or an efference copy of motor programs. Surprisingly, AB neurons are active during the early but not later exploration of an intruder although exploration includes sniffing that enables access to pheromones. Early exploration may involve behaviors that are hard to detect, or the response of AB neurons to sniffing may be suppressed during later exploration.

Our studies suggest a model for why $Trpc2^{-/-}$ males mate with both sexes. The activity of male $Trpc2^{-/-}$ AB neurons mis-identifies males as females, leading to indiscriminate mating and a loss of fighting. The source of this signal is likely to be the MOE, because AB neurons respond to pheromones in $Trpc2^{-/-}$ males. Accordingly, disrupting AB neurons precludes relay of this MOE-derived signal and essentially abrogates mating and fighting, mirroring the phenotype of males with genetically disabled MOE function (Mandiyan et al., 2005; Wang et al., 2006; Yoon et al., 2005). Both the MOE and VNO regulate social behaviors (Keller et al., 2009), and our results show that male AB neurons shape sex recognition and social behaviors likely by processing signals from both MOE and VNO.

Sex Differences in the Function of AB Neurons

We find that female AB neurons do not appear to recognize sex or contribute to behavioral output. The function of these cells may have been hard to discern in our assays or our perturbations may have been inadequate. Nevertheless, similar perturbations in males revealed important functions of AB

(J) No significant change in percent males mating with optogenetic inhibition of AB neurons.
(K and L) Optogenetic inhibition of AB neurons reduces mounts per assay (K) and increases latency to mount, intromit, and ejaculate (L).
(M–P) Brief (90 s) laser illumination of $ChR2^+$ AB neurons in resident males interacting with WT intruder males for 15 min (M).
(N) Laser illumination eliminates attacks and promotes mounting.
(O) Laser illumination reduces attacks and increases mounts per assay.
(P) Latency to mount intruder male is similar to latency to mount receptive female intruder (shown by horizontal dashed line). Data for males mating with females is from (H).
Mean ± SEM; n = 8 (A–H), 8 (I–L), 5 (M–P). *$p < 0.05$, **$p < 0.01$.
See also Figure S7 and Video S5.

neurons. More likely, the observed functional sex differences in AB neurons reflect dimorphisms in local or long distance circuit computation. In any event, the two sexes appear to employ dimorphic neural substrates to distinguish between and interact with males and females.

We have identified many differences between male and female AB neurons under sex-typical hormonal conditions. Whether these dimorphisms are developmentally hard-wired or reflect circulating hormones in adults (Becker et al., 2005) is unclear. Given the importance of aromatase in sexual differentiation and social behaviors, its function in AB neurons should be explored in future studies.

AB Neurons Distinguish between the Sexes and Enable Social Interactions in Sexually Naive Males

In contrast to male AB neurons, male MeA and VMHvl neurons reliably report sex of conspecifics only following experience with females (Li et al., 2017; Remedios et al., 2017), and stimulation of these (or POA) neurons elicits time-locked behaviors (Hong et al., 2014; Lee et al., 2014; Wei et al., 2018). Thus, the neural pathway underlying innate sex recognition may be distinct from that which regulates mating or fighting. This is analogous to models for parallel visual processing of "where" and "what" functions for object localization (Nassi and Callaway, 2009; Seabrook et al., 2017). Male AB neurons may encode "which sex" whereas MeA and VMHvl neurons may encode "how to act" with that sex. This model does not preclude cross-talk or additional distributive processing of social behaviors. Alternatively, a hierarchical pathway may underlie social behaviors such that AB neurons report biological sex to guide behavioral choice, and MeA, VMHvl, and POA neurons read out activity of AB neurons to enact distinct motor programs of social behavior.

Momentary activation of male AB neurons promotes a bias to mate rather than fight and appears to render ineffective incoming input about aggression-eliciting male cues. If sexual identification of individuals initiates a decision about how to interact with them, our findings show that this decision is reached quickly, enacted after a brief delay, and seems impervious to additional sensory evidence. It will be fascinating to understand mechanisms underlying this enduring cognitive state that guides social behaviors.

STAR★METHODS

Detailed methods are provided in the online version of this paper and include the following:

- KEY RESOURCES TABLE
- CONTACT FOR REAGENT AND RESOURCE SHARING
- EXPERIMENTAL MODEL AND SUBJECT DETAILS
  - Mice
- METHOD DETAILS
  - Viruses
  - Stereotaxic surgery
  - Histology
  - Slice imaging
  - Fiber Photometry
  - Chemogenetic inhibition
  - Caspase-3 mediated ablation
  - Optogenetic manipulation
  - Hormone priming
  - Hormone assays
  - Behavioral testing
- QUANTIFICATION AND STATISTICAL ANALYSIS

SUPPLEMENTAL INFORMATION

Supplemental Information includes seven figures, one table, and five videos and can be found with this article online at https://doi.org/10.1016/j.cell.2018.12.041.

ACKNOWLEDGMENTS

We thank Thomas Clandinin, Karl Deisseroth, Liqun Luo, Kristin Scott, Tom Südhof, and the Shah lab for discussions and Yiming Chen for input on photometry. This work was supported by grants from NIH (R01NS049488 and R01NS083872) to N.M.S.

AUTHOR CONTRIBUTIONS

Conceptualization, D.W.B. and N.M.S.; Funding, N.M.S.; Investigation, A.A.T.S., A.L., D.W.B., M.M.M., and T.Y.; Supervision, D.W.B. and N.M.S.; Writing, D.W.B. and N.M.S.

DECLARATION OF INTERESTS

The authors declare no competing interests.

Received: September 14, 2018
Revised: November 13, 2018
Accepted: December 21, 2018
Published: January 31, 2019

REFERENCES

Arnold, A.P. (2009). The organizational-activational hypothesis as the foundation for a unified theory of sexual differentiation of all mammalian tissues. Horm. Behav. *55*, 570–578.

Baum, M.J., and Bakker, J. (2013). Roles of sex and gonadal steroids in mammalian pheromonal communication. Front. Neuroendocrinol. *34*, 268–284.

Becker, J.B., Arnold, A.P., Berkley, K.J., Blaustein, J.D., Eckel, L.A., Hampson, E., Herman, J.P., Marts, S., Sadee, W., Steiner, M., et al. (2005). Strategies and methods for research on sex differences in brain and behavior. Endocrinology *146*, 1650–1673.

Ben-Shaul, Y., Katz, L.C., Mooney, R., and Dulac, C. (2010). In vivo vomeronasal stimulation reveals sensory encoding of conspecific and allospecific cues by the mouse accessory olfactory bulb. Proc. Natl. Acad. Sci. USA *107*, 5172–5177.

Brennan, P.A., Schellinck, H.M., and Keverne, E.B. (1999). Patterns of expression of the immediate-early gene egr-1 in the accessory olfactory bulb of female mice exposed to pheromonal constituents of male urine. Neuroscience *90*, 1463–1470.

Broadwell, R.D. (1975). Olfactory relationships of the telencephalon and diencephalon in the rabbit. I. An autoradiographic study of the efferent connections of the main and accessory olfactory bulbs. J. Comp. Neurol. *163*, 329–345.

Chamero, P., Marton, T.F., Logan, D.W., Flanagan, K., Cruz, J.R., Saghatelian, A., Cravatt, B.F., and Stowers, L. (2007). Identification of protein pheromones that promote aggressive behaviour. Nature *450*, 899–902.

Chen, Y., Lin, Y.-C., Kuo, T.-W., and Knight, Z.A. (2015). Sensory detection of food rapidly modulates arcuate feeding circuits. Cell *160*, 829–841.

Claro, F., Segovia, S., Guilamón, A., and Del Abril, A. (1995). Lesions in the medial posterior region of the BST impair sexual behavior in sexually experienced and inexperienced male rats. Brain Res. Bull. *36*, 1–10.

Connor, J. (1972). Olfactory control of aggressive and sexual behavior in the mouse (Mus musculus L.). Psychon. Sci. *27*, 1–3.

Cooke, B.M., and Simerly, R.B. (2005). Ontogeny of bidirectional connections between the medial nucleus of the amygdala and the principal bed nucleus of the stria terminalis in the rat. J. Comp. Neurol. *489*, 42–58.

Crawley, J.N., Schleidt, W.M., and Contrera, J.F. (1975). Does social environment decrease propensity to fight in male mice? Behav. Biol. *15*, 73–83.

Crestani, C.C., Alves, F.H., Gomes, F.V., Resstel, L.B., Correa, F.M., and Herman, J.P. (2013). Mechanisms in the bed nucleus of the stria terminalis involved in control of autonomic and neuroendocrine functions: a review. Curr. Neuropharmacol. *11*, 141–159.

Cui, G., Jun, S.B., Jin, X., Pham, M.D., Vogel, S.S., Lovinger, D.M., and Costa, R.M. (2013). Concurrent activation of striatal direct and indirect pathways during action initiation. Nature *494*, 238–242.

Davis, B.J., Macrides, F., Youngs, W.M., Schneider, S.P., and Rosene, D.L. (1978). Efferents and centrifugal afferents of the main and accessory olfactory bulbs in the hamster. Brain Res. Bull. *3*, 59–72.

Dong, H.-W., and Swanson, L.W. (2004). Projections from bed nuclei of the stria terminalis, posterior division: implications for cerebral hemisphere regulation of defensive and reproductive behaviors. J. Comp. Neurol. *471*, 396–433.

Emery, D.E., and Sachs, B.D. (1976). Copulatory behavior in male rats with lesions in the bed nucleus of the stria terminalis. Physiol. Behav. *17*, 803–806.

Fenno, L., Yizhar, O., and Deisseroth, K. (2011). The development and application of optogenetics. Annu. Rev. Neurosci. *34*, 389–412.

Ferrero, D.M., Lemon, J.K., Fluegge, D., Pashkovski, S.L., Korzan, W.J., Datta, S.R., Spehr, M., Fendt, M., and Liberles, S.D. (2011). Detection and avoidance of a carnivore odor by prey. Proc. Natl. Acad. Sci. USA *108*, 11235–11240.

Fisher, C.R., Graves, K.H., Parlow, A.F., and Simpson, E.R. (1998). Characterization of mice deficient in aromatase (ArKO) because of targeted disruption of the cyp19 gene. Proc. Natl. Acad. Sci. USA *95*, 6965–6970.

Fu, X., Yan, Y., Xu, P.S., Geerlof-Vidavsky, I., Chong, W., Gross, M.L., and Holy, T.E. (2015). A molecular code for identity in the vomeronasal system. Cell *163*, 313–323.

Gammie, S.C., and Nelson, R.J. (2001). cFOS and pCREB activation and maternal aggression in mice. Brain Res. *898*, 232–241.

Gandelman, R. (1972). Mice: postpartum aggression elicited by the presence of an intruder. Horm. Behav. *3*, 23–28.

Giardino, W.J., Eban-Rothschild, A., Christoffel, D.J., Li, S.-B., Malenka, R.C., and de Lecea, L. (2018). Parallel circuits from the bed nuclei of stria terminalis to the lateral hypothalamus drive opposing emotional states. Nat. Neurosci. *21*, 1084–1095.

Gu, G., Cornea, A., and Simerly, R.B. (2003). Sexual differentiation of projections from the principal nucleus of the bed nuclei of the stria terminalis. J. Comp. Neurol. *460*, 542–562.

Guillamón, A., Segovia, S., and del Abril, A. (1988). Early effects of gonadal steroids on the neuron number in the medial posterior region and the lateral division of the bed nucleus of the stria terminalis in the rat. Brain Res. Dev. Brain Res. *44*, 281–290.

Gunaydin, L.A., Grosenick, L., Finkelstein, J.C., Kauvar, I.V., Fenno, L.E., Adhikari, A., Lammel, S., Mirzabekov, J.J., Airan, R.D., Zalocusky, K.A., et al. (2014). Natural neural projection dynamics underlying social behavior. Cell *157*, 1535–1551.

Haga-Yamanaka, S., Ma, L., He, J., Qiu, Q., Lavis, L.D., Looger, L.L., and Yu, C.R. (2014). Integrated action of pheromone signals in promoting courtship behavior in male mice. eLife *3*, e03025.

Halem, H.A., Cherry, J.A., and Baum, M.J. (1999). Vomeronasal neuroepithelium and forebrain Fos responses to male pheromones in male and female mice. J. Neurobiol. *39*, 249–263.

Hammen, G.F., Turaga, D., Holy, T.E., and Meeks, J.P. (2014). Functional organization of glomerular maps in the mouse accessory olfactory bulb. Nat. Neurosci. *17*, 953–961.

Hashikawa, K., Hashikawa, Y., Tremblay, R., Zhang, J., Feng, J.E., Sabol, A., Piper, W.T., Lee, H., Rudy, B., and Lin, D. (2017). Esr1^{+} cells in the ventromedial hypothalamus control female aggression. Nat. Neurosci. *20*, 1580–1590.

He, J., Ma, L., Kim, S., Nakai, J., and Yu, C.R. (2008). Encoding gender and individual information in the mouse vomeronasal organ. Science *320*, 535–538.

Holy, T.E. (2018). The accessory olfactory system: innately specialized or microcosm of mammalian circuitry? Annu. Rev. Neurosci. *41*, 501–525.

Holy, T.E., Dulac, C., and Meister, M. (2000). Responses of vomeronasal neurons to natural stimuli. Science *289*, 1569–1572.

Honda, S., Harada, N., Ito, S., Takagi, Y., and Maeda, S. (1998). Disruption of sexual behavior in male aromatase-deficient mice lacking exons 1 and 2 of the cyp19 gene. Biochem. Biophys. Res. Commun. *252*, 445–449.

Hong, W., Kim, D.-W., and Anderson, D.J. (2014). Antagonistic control of social versus repetitive self-grooming behaviors by separable amygdala neuronal subsets. Cell *158*, 1348–1361.

Isogai, Y., Si, S., Pont-Lezica, L., Tan, T., Kapoor, V., Murthy, V.N., and Dulac, C. (2011). Molecular organization of vomeronasal chemoreception. Nature *478*, 241–245.

Kang, N., Baum, M.J., and Cherry, J.A. (2009). A direct main olfactory bulb projection to the 'vomeronasal' amygdala in female mice selectively responds to volatile pheromones from males. Eur. J. Neurosci. *29*, 624–634.

Kang, N., McCarthy, E.A., Cherry, J.A., and Baum, M.J. (2011a). A sex comparison of the anatomy and function of the main olfactory bulb-medial amygdala projection in mice. Neuroscience *172*, 196–204.

Kang, N., Baum, M.J., and Cherry, J.A. (2011b). Different profiles of main and accessory olfactory bulb mitral/tufted cell projections revealed in mice using an anterograde tracer and a whole-mount, flattened cortex preparation. Chem. Senses *36*, 251–260.

Keller, M., Baum, M.J., Brock, O., Brennan, P.A., and Bakker, J. (2009). The main and the accessory olfactory systems interact in the control of mate recognition and sexual behavior. Behav. Brain Res. *200*, 268–276.

Kimoto, H., Haga, S., Sato, K., and Touhara, K. (2005). Sex-specific peptides from exocrine glands stimulate mouse vomeronasal sensory neurons. Nature *437*, 898–901.

Kimoto, H., Sato, K., Nodari, F., Haga, S., Holy, T.E., and Touhara, K. (2007). Sex- and strain-specific expression and vomeronasal activity of mouse ESP family peptides. Curr. Biol. *17*, 1879–1884.

King, J.A. (1957). Relationships between early social experience and adult aggressive behavior in inbred mice. J. Genet. Psychol. *90*, 151–166.

Lee, H., Kim, D.-W., Remedios, R., Anthony, T.E., Chang, A., Madisen, L., Zeng, H., and Anderson, D.J. (2014). Scalable control of mounting and attack by Esr1+ neurons in the ventromedial hypothalamus. Nature *509*, 627–632.

Lehman, M.N., Powers, J.B., and Winans, S.S. (1983). Stria terminalis lesions alter the temporal pattern of copulatory behavior in the male golden hamster. Behav. Brain Res. *8*, 109–128.

Lephart, E.D. (1996). A review of brain aromatase cytochrome P450. Brain Res. Brain Res. Rev. *22*, 1–26.

Leypold, B.G., Yu, C.R., Leinders-Zufall, T., Kim, M.M., Zufall, F., and Axel, R. (2002). Altered sexual and social behaviors in trp2 mutant mice. Proc. Natl. Acad. Sci. USA *99*, 6376–6381.

Li, Y., Mathis, A., Grewe, B.F., Osterhout, J.A., Ahanonu, B., Schnitzer, M.J., Murthy, V.N., and Dulac, C. (2017). Neuronal representation of social information in the medial amygdala of awake behaving mice. Cell *171*, 1176–1190.

Liberles, S.D. (2014). Mammalian pheromones. Annu. Rev. Physiol. *76*, 151–175.

Liberles, S.D. (2015). Trace amine-associated receptors: ligands, neural circuits, and behaviors. Curr. Opin. Neurobiol. *34*, 1–7.

Liu, Y.C., Salamone, J.D., and Sachs, B.D. (1997). Lesions in medial preoptic area and bed nucleus of stria terminalis: differential effects on copulatory behavior and noncontact erection in male rats. J. Neurosci. *17*, 5245–5253.

Luo, M., Fee, M.S., and Katz, L.C. (2003). Encoding pheromonal signals in the accessory olfactory bulb of behaving mice. Science *299*, 1196–1201.

Mandiyan, V.S., Coats, J.K., and Shah, N.M. (2005). Deficits in sexual and aggressive behaviors in Cnga2 mutant mice. Nat. Neurosci. *8*, 1660–1662.

Maruniak, J.A., Wysocki, C.J., and Taylor, J.A. (1986). Mediation of male mouse urine marking and aggression by the vomeronasal organ. Physiol. Behav. *37*, 655–657.

Matsumoto, T., Honda, S., and Harada, N. (2003). Alteration in sex-specific behaviors in male mice lacking the aromatase gene. Neuroendocrinology *77*, 416–424.

McCarthy, M.M. (2008). Estradiol and the developing brain. Physiol. Rev. *88*, 91–124.

Meeks, J.P., Arnson, H.A., and Holy, T.E. (2010). Representation and transformation of sensory information in the mouse accessory olfactory system. Nat. Neurosci. *13*, 723–730.

Moga, M.M., Saper, C.B., and Gray, T.S. (1989). Bed nucleus of the stria terminalis: cytoarchitecture, immunohistochemistry, and projection to the parabrachial nucleus in the rat. J. Comp. Neurol. *283*, 315–332.

Morgan, C.W., Julien, O., Unger, E.K., Shah, N.M., and Wells, J.A. (2014). Turning on caspases with genetics and small molecules. Methods Enzymol. *544*, 179–213.

Naftolin, F., Ryan, K.J., and Petro, Z. (1971). Aromatization of androstenedione by limbic system tissue from human foetuses. J. Endocrinol. *51*, 795–796.

Nassi, J.J., and Callaway, E.M. (2009). Parallel processing strategies of the primate visual system. Nat. Rev. Neurosci. *10*, 360–372.

Nelson, R.J., and Trainor, B.C. (2007). Neural mechanisms of aggression. Nat. Rev. Neurosci. *8*, 536–546.

Ng, L., Bernard, A., Lau, C., Overly, C.C., Dong, H.-W., Kuan, C., Pathak, S., Sunkin, S.M., Dang, C., Bohland, J.W., et al. (2009). An anatomic gene expression atlas of the adult mouse brain. Nat. Neurosci. *12*, 356–362.

Nodari, F., Hsu, F.-F., Fu, X., Holekamp, T.F., Kao, L.-F., Turk, J., and Holy, T.E. (2008). Sulfated steroids as natural ligands of mouse pheromone-sensing neurons. J. Neurosci. *28*, 6407–6418.

O'Connell, R.J., and Meredith, M. (1984). Effects of volatile and nonvolatile chemical signals on male sex behaviors mediated by the main and accessory olfactory systems. Behav. Neurosci. *98*, 1083–1093.

Omura, M., and Mombaerts, P. (2014). Trpc2-expressing sensory neurons in the main olfactory epithelium of the mouse. Cell Rep. *8*, 583–595.

Pankevich, D.E., Baum, M.J., and Cherry, J.A. (2004). Olfactory sex discrimination persists, whereas the preference for urinary odorants from estrous females disappears in male mice after vomeronasal organ removal. J. Neurosci. *24*, 9451–9457.

Pankevich, D.E., Cherry, J.A., and Baum, M.J. (2006). Effect of vomeronasal organ removal from male mice on their preference for and neural Fos responses to female urinary odors. Behav. Neurosci. *120*, 925–936.

Pfaus, J.G., and Heeb, M.M. (1997). Implications of immediate-early gene induction in the brain following sexual stimulation of female and male rodents. Brain Res. Bull. *44*, 397–407.

Powers, J.B., Newman, S.W., and Bergondy, M.L. (1987). MPOA and BNST lesions in male Syrian hamsters: differential effects on copulatory and chemoinvestigatory behaviors. Behav. Brain Res. *23*, 181–195.

Ramos, S.M., and DeBold, J.F. (2000). Fos expression in female hamsters after various stimuli associated with mating. Physiol. Behav. *70*, 557–566.

Remedios, R., Kennedy, A., Zelikowsky, M., Grewe, B.F., Schnitzer, M.J., and Anderson, D.J. (2017). Social behaviour shapes hypothalamic neural ensemble representations of conspecific sex. Nature *550*, 388–392.

Sam, M., Vora, S., Malnic, B., Ma, W., Novotny, M.V., and Buck, L.B. (2001). Neuropharmacology. Odorants may arouse instinctive behaviours. Nature *412*, 142.

Scott, J.P. (1966). Agonistic behavior of mice and rats: a review. Am. Zool. *6*, 683–701.

Seabrook, T.A., Burbridge, T.J., Crair, M.C., and Huberman, A.D. (2017). Architecture, function, and assembly of the mouse visual system. Annu. Rev. Neurosci. *40*, 499–538.

Segovia, S., and Guillamón, A. (1993). Sexual dimorphism in the vomeronasal pathway and sex differences in reproductive behaviors. Brain Res. Brain Res. Rev. *18*, 51–74.

Shah, N.M., Pisapia, D.J., Maniatis, S., Mendelsohn, M.M., Nemes, A., and Axel, R. (2004). Visualizing sexual dimorphism in the brain. Neuron *43*, 313–319.

Simerly, R.B. (2002). Wired for reproduction: organization and development of sexually dimorphic circuits in the mammalian forebrain. Annu. Rev. Neurosci. *25*, 507–536.

Stack, E.C., Balakrishnan, R., Numan, M.J., and Numan, M. (2002). A functional neuroanatomical investigation of the role of the medial preoptic area in neural circuits regulating maternal behavior. Behav. Brain Res. *131*, 17–36.

Sternson, S.M., and Roth, B.L. (2014). Chemogenetic tools to interrogate brain functions. Annu. Rev. Neurosci. *37*, 387–407.

Stowers, L., Holy, T.E., Meister, M., Dulac, C., and Koentges, G. (2002). Loss of sex discrimination and male-male aggression in mice deficient for TRP2. Science *295*, 1493–1500.

Südhof, T.C. (2015). Reproducibility: experimental mismatch in neural circuits. Nature *528*, 338–339.

Swanson, L.W. (2000). Cerebral hemisphere regulation of motivated behavior. Brain Res. *886*, 113–164.

Takahashi, A., and Miczek, K.A. (2014). Neurogenetics of aggressive behavior: studies in rodents. Curr. Top Behav. Neurosci. *17*, 3–44.

Tamamaki, N., Yanagawa, Y., Tomioka, R., Miyazaki, J., Obata, K., and Kaneko, T. (2003). Green fluorescent protein expression and colocalization with calretinin, parvalbumin, and somatostatin in the GAD67-GFP knock-in mouse. J. Comp. Neurol. *467*, 60–79.

Thompson, M.L., and Edwards, D.A. (1971). Experiential and strain determinants of the estrogen-progesterone induction of sexual receptivity in spayed female mice. Horm. Behav. *2*, 299–305.

Toda, K., Saibara, T., Okada, T., Onishi, S., and Shizuta, Y. (2001). A loss of aggressive behaviour and its reinstatement by oestrogen in mice lacking the aromatase gene (Cyp19). J. Endocrinol. *168*, 217–220.

Tolokh, I.I., Fu, X., and Holy, T.E. (2013). Reliable sex and strain discrimination in the mouse vomeronasal organ and accessory olfactory bulb. J. Neurosci. *33*, 13903–13913.

Trinh, K., and Storm, D.R. (2003). Vomeronasal organ detects odorants in absence of signaling through main olfactory epithelium. Nat. Neurosci. *6*, 519–525.

Unger, E.K., Burke, K.J., Jr., Yang, C.F., Bender, K.J., Fuller, P.M., and Shah, N.M. (2015). Medial amygdalar aromatase neurons regulate aggression in both sexes. Cell Rep. *10*, 453–462.

Valcourt, R.J., and Sachs, B.D. (1979). Penile reflexes and copulatory behavior in male rats following lesions in the bed nucleus of the stria terminalis. Brain Res. Bull. *4*, 131–133.

von Campenhausen, H., and Mori, K. (2000). Convergence of segregated pheromonal pathways from the accessory olfactory bulb to the cortex in the mouse. Eur. J. Neurosci. *12*, 33–46.

Vong, L., Ye, C., Yang, Z., Choi, B., Chua, S., Jr., and Lowell, B.B. (2011). Leptin action on GABAergic neurons prevents obesity and reduces inhibitory tone to POMC neurons. Neuron *71*, 142–154.

Walker, D.L., Toufexis, D.J., and Davis, M. (2003). Role of the bed nucleus of the stria terminalis versus the amygdala in fear, stress, and anxiety. Eur. J. Pharmacol. *463*, 199–216.

Wang, Z., Balet Sindreu, C., Li, V., Nudelman, A., Chan, G.C.-K., and Storm, D.R. (2006). Pheromone detection in male mice depends on signaling through

the type 3 adenylyl cyclase in the main olfactory epithelium. J. Neurosci. *26*, 7375–7379.

Wei, Y.-C., Wang, S.-R., Jiao, Z.-L., Zhang, W., Lin, J.-K., Li, X.-Y., Li, S.-S., Zhang, X., and Xu, X.-H. (2018). Medial preoptic area in mice is capable of mediating sexually dimorphic behaviors regardless of gender. Nat. Commun. *9*, 279.

Wersinger, S.R., Sannen, K., Villalba, C., Lubahn, D.B., Rissman, E.F., and De Vries, G.J. (1997). Masculine sexual behavior is disrupted in male and female mice lacking a functional estrogen receptor alpha gene. Horm. Behav. *32*, 176–183.

Wu, M.V., Manoli, D.S., Fraser, E.J., Coats, J.K., Tollkuhn, J., Honda, S., Harada, N., and Shah, N.M. (2009). Estrogen masculinizes neural pathways and sex-specific behaviors. Cell *139*, 61–72.

Xu, X., Coats, J.K., Yang, C.F., Wang, A., Ahmed, O.M., Alvarado, M., Izumi, T., and Shah, N.M. (2012). Modular genetic control of sexually dimorphic behaviors. Cell *148*, 596–607.

Yang, C.F., and Shah, N.M. (2014). Representing sex in the brain, one module at a time. Neuron *82*, 261–278.

Yang, C.F., Chiang, M.C., Gray, D.C., Prabhakaran, M., Alvarado, M., Juntti, S.A., Unger, E.K., Wells, J.A., and Shah, N.M. (2013). Sexually dimorphic neurons in the ventromedial hypothalamus govern mating in both sexes and aggression in males. Cell *153*, 896–909.

Yang, T., Yang, C.F., Chizari, M.D., Maheswaranathan, N., Burke, K.J., Jr., Borius, M., Inoue, S., Chiang, M.C., Bender, K.J., Ganguli, S., and Shah, N.M. (2017). Social control of hypothalamus-mediated male aggression. Neuron *95*, 955–970.

Yao, S., Bergan, J., Lanjuin, A., and Dulac, C. (2017). Oxytocin signaling in the medial amygdala is required for sex discrimination of social cues. eLife *6*, e31373.

Yoon, H., Enquist, L.W., and Dulac, C. (2005). Olfactory inputs to hypothalamic neurons controlling reproduction and fertility. Cell *123*, 669–682.

Zardetto-Smith, A.M., Beltz, T.G., and Johnson, A.K. (1994). Role of the central nucleus of the amygdala and bed nucleus of the stria terminalis in experimentally-induced salt appetite. Brain Res. *645*, 123–134.

Zhou, J.N., Hofman, M.A., Gooren, L.J., and Swaab, D.F. (1995). A sex difference in the human brain and its relation to transsexuality. Nature *378*, 68–70.

STAR★METHODS

KEY RESOURCES TABLE

REAGENT or RESOURCE	SOURCE	IDENTIFIER
Antibodies		
Sheep anti-GFP	Biorad	Cat # 4745-1051; RRID: AB_619712
Rat anti-RFP	Chromotek	Cat # 5f8-100; RRID: AB_2336064
Chicken anti- β-galactosidase	Abcam	Cat # 9361; RRID: AB_307210
Rabbit anti-Fos	EMD Millipore	Cat # PC38; RRID: AB_2106755
Donkey anti-sheep, Alexa 488 conjugate	Jackson ImmunoResearch	Cat # 713-545-147; RRID: AB_2340745
Donkey anti-rat, Cy3 conjugate	Jackson ImmunoResearch	Cat # 712-165-150; RRID: AB_2340666
Donkey anti-chicken, Alexa 488 conjugate	Jackson ImmunoResearch	Cat # 703-545-155; RRID: AB_2340375
Donkey anti-chicken, Cy3 conjugate	Jackson ImmunoResearch	Cat # 703-165-155; RRID: AB_2340363
Donkey anti-chicken, Alexa 647 conjugate	Jackson ImmunoResearch	Cat # 703-605-155; RRID: AB_2340379
Donkey anti-rabbit, Cy3 conjugate	Jackson ImmunoResearch	Cat # 711-165-152; RRID: AB_2307443
Bacterial and Virus Strains		
Recombinant adeno-associated virus: AAV1-Syn-flex-GCaMP6s	Penn Vector Core	Addgene number: 100845
Recombinant adeno-associated virus: AAV1-EF1α-flex-hChR2(H134R):eYFP	Penn Vector Core	Addgene number: 20298
Recombinant adeno-associated virus: AAV1-EF1α-flex-eNpHR3.0:eYFP	Penn Vector Core	Addgene number: 26966
Recombinant adeno-associated virus: AAV1-CAG-flex-eGFP	Penn Vector Core	Addgene number: 59331
Recombinant adeno-associated virus: AAV1-EF1α-taCasp3-TEVp	UNC Vector Core	Addgene number: 45580
Recombinant adeno-associated virus: AAV1-EF1α-flex-hM4DGi:mCherry	UNC Vector Core	Addgene number: 50461
Recombinant adeno-associated virus: AAV5-EF1α-flex-mCherry	UNC Vector Core	Addgene number: 50462
Recombinant adeno-associated virus: AAV1-EF1α-flex-eYFP	UNC Vector Core	Addgene number: 27056
Chemicals, Peptides, and Recombinant Proteins		
DAPI	Sigma-Aldrich	Cat # D9542; CAS 28718-90-3
Clozapine-N-oxide (CNO)	Enzo Life Sciences	Cat # BML-NS105-0005
Estradiol	Sigma-Aldrich	Cat # E8875;CAS 50-28-2
Progesterone	Sigma-Aldrich	Cat # P0130; CAS 57-83-0
2-phenylethylamine (PEA)	Sigma-Aldrich	Cat # 128945; CAS 64-04-0
Cadaverine	Sigma-Aldrich	Cat # D22606; CAS 462-94-2
Critical Commercial Assays		
Testosterone ELISA kit	Cayman	Cat # 582701
Experimental Models: Organisms/Strains		
Mouse: C57BL/6J	The Jackson Laboratory	Cat # 000664; RRID: IMSR_JAX:000664
Mouse: C57BL/6N	Charles River	Cat # 027
Mouse: Swiss Webster	Charles River	Cat # 024
Mouse: 129/SvEvTac	Taconic Biosciences	Cat # 129SVE-M
Mouse: *Aro*^{Cre}	Unger et al., 2015	Cat # 027038; RRID: IMSR_JAX:027038
Mouse: *Aro*^{IPIN}	Wu et al., 2009	Cat # 012377; RRID: IMSR_JAX:012377
Mouse: *Trpc2*$^{-/-}$	Leypold et al., 2002	N/A

(*Continued on next page*)

Continued

REAGENT or RESOURCE	SOURCE	IDENTIFIER
Mouse: *Vgat*^{Cre}	Vong et al., 2011	Cat # 028862; RRID: IMSR_JAX:028862
Mouse: *Gad1*^{EGFP}	Tamamaki et al., 2003	N/A
Software and Algorithms		
ImageJ	NIH	https://imagej.nih.gov/ij/index.html; RRID: SCR_003070
MATLAB	MathWorks	https://www.mathworks.com/products.html; RRID: SCR_001622
GraphPad Prism 6	GraphPad Software	https://www.graphpad.com/scientific-software/prism/; RRID: SCR_002798

CONTACT FOR REAGENT AND RESOURCE SHARING

Further information and requests for resources and reagents should be directed to and will be fulfilled by the Lead Contact, Nirao M. Shah (nirao@stanford.edu).

EXPERIMENTAL MODEL AND SUBJECT DETAILS

Mice

Animal studies were conducted following Institutional Animal Care and Use Committee guidelines and protocols. Adult mice 10-24 weeks of age were used for all studies. Mice were bred in our colony (*Aro*$^{Cre/IPIN}$, *Aro*^{IPIN}, *Trpc2*$^{-/-}$, *Vgat*^{Cre}, and *Gad1*^{EGFP}) (Leypold et al., 2002; Tamamaki et al., 2003; Unger et al., 2015; Vong et al., 2011; Wu et al., 2009) or purchased from Jackson (C57BL/6J for WT females), Taconic (129/SvEvTac for WT males), and Charles River (C57BL/6N for tests of WT sexually naive inter-male aggression shown in Figures S1I–S1K). *Aro*$^{Cre/IPIN}$ mice harbor Cre recombinase and nuclear LacZ (Unger et al., 2015; Wu et al., 2009) inserted 3′ of IRES elements separately into the 3′UTR of aromatase in a gene conserving manner. Mice were housed under a 12:12 hr light:dark cycle, and water and food were available *ad libitum* unless otherwise mentioned. Mice were group housed by sex after weaning at 3 weeks of age and were therefore sexually naive prior to initiation of behavioral testing unless otherwise mentioned. Recent findings indicate that Swiss Webster (SW) females display maternal aggression more reliably than the C57BL/6J background in which *Aro*$^{Cre/IPIN}$ mice are maintained (Hashikawa et al., 2017). To test whether we would observe comparable or different phenotypes in females from this more aggressive strain, we backcrossed the *Aro*$^{Cre/IPIN}$ alleles into the SW background > 3 times and subsequently assayed cohorts of these females for all studies in which female C57BL/6J mice had also been tested. Indeed, we did observe more maternal aggression in SW compared to C57BL/6J females (Table S1). However, all significant differences observed were seen in both strains, and there were no differences in the effects of our functional manipulations between the strains; therefore, we have provided data for SW and C57BL/6J females separately in Table S1 and combined data from both strains for graphical presentation in the figures.

METHOD DETAILS

Viruses

AAV-Syn-flex-GCaMP6s, AAV-EF1α-flex-hChR2(H134R):eYFP, AAV-EF1α-flex-eNpHR3.0:eYFP, and AAV-CAG-flex-eGFP were purchased from the Penn Vector Core. AAV-EF1α-taCasp3-TEVp, AAV-EF1α-flex-hM4DGi:mCherry, AAV-EF1α-flex-mCherry, and AAV-EF1α-flex-eYFP were purchased from the UNC Vector Core or custom packaged by the UNC Vector Core with plasmid DNA from our stocks or purchased from Addgene. All virus titers were > 10^{12} genomic copies/mL.

Stereotaxic surgery

Viruses were delivered into brains of male and female mice at 10-16 weeks of age as described previously (Yang et al., 2013). Viruses were injected into empirically determined coordinates for the BNSTpr (±0.85 mm mediolateral, −0.20 mm anteroposterior, and −4.30 mm dorsoventral relative to bregma). For fiber photometry studies, 0.8 μl of virus was injected unilaterally (counterbalanced for injections into left or right hemisphere across animals), and for all functional manipulation studies, 0.8 μl of virus was injected bilaterally. Following viral injection during the same surgery, mice used for fiber photometry and optogenetic manipulation studies were implanted with an optic fiber 0.5 mm dorsal to the viral injection into the BNSTpr such that the optic fiber was extracranially housed in a ceramic cannula. For optogenetic studies, optic fibers were implanted bilaterally over the BNSTpr. The cannula was secured to the skull using adhesive dental cement (Parkell Inc). In addition, female mice used for mating assays were ovariectomized during the stereotaxic surgery while the virus was being delivered. Following surgery, mice were allowed to recover individually over a heat pad and then returned to their home cages.

Histology

We confirmed expression of virally delivered genes in all experimental animals using previously published procedures (Yang et al., 2013). We consistently achieved reliable infection of AB neurons, and we did not observe infection of other brain areas expressing aromatase including the POA and MeA. For histological analysis following behavioral testing, mice were perfused with 4% paraformaldehyde (PFA) and brains were dissected and post-fixed in 4% PFA overnight. Brains were sectioned at 65 μm using a vibrating microtome (Leica) and then immunolabeled as described previously (Yang et al., 2013). The primary antisera used were: sheep anti-GFP (Biorad; 1:2000), rat anti-RFP (Chromotek; 1:2000), chicken anti-β-galactosidase (Abcam; 1:3000), and rabbit anti-Fos (Calbiochem; 1:2000). The fluorophore conjugated secondary antisera used were: Alexa Fluor 488 donkey anti-sheep (Jackson ImmunoResearch; 1:300), Cy3 donkey anti-rat (Jackson ImmunoResearch; 1:800), Alexa Fluor 488 donkey anti-chicken (Jackson ImmunoResearch; 1:300), Cy3 donkey anti-chicken (Jackson ImmunoResearch; 1:800), Alexa Fluor 647 donkey anti-chicken (Jackson ImmunoResearch; 1:500), and Cy3 donkey anti-rabbit (Jackson ImmunoResearch; 1:800). Sections were also counterstained with DAPI (0.2 μg/ml). Optic fiber placement above the BNSTpr was verified for all mice used in fiber photometry and optogenetic manipulation studies, and Fos induction by ChR2 was confirmed by immunostaining for Fos in mice perfused 1 hr after 5 min of laser illumination (473nm, 5Hz, 5ms pulse width, 30 s cycles, 2mW). Immunolabeled sections were imaged via confocal microscopy (Zeiss) and quantified using ImageJ software as described previously (Unger et al., 2015; Wu et al., 2009).

Slice imaging

Acute slice preparation

Slices through the BNSTpr were prepared from male and female Aro^{Cre} mice in whom an AAV encoding Cre-dependent GCaMP6s or control eGFP had been delivered into the BNSTpr 4 weeks prior to slice preparation. Mice were euthanized, and brains were dissected out and sectioned at 300 μm in ice-cold oxygenated (95% O_2/5% CO_2) saline containing 26mM $NaHCO_3$, 1.25 mM NaH_2PO_4, 3 mM KCl, 10 mM glucose, 210 mM sucrose, 2 mM $CaCl_2$, 2 mM $MgCl_2$. Slices were then transferred to oxygenated artificial cerebrospinal fluid (aCSF) containing 125 mM NaCl, 25 mM $NaHCO_3$, 1.25 mM NaH_2PO_4, 4 mM KCl, 15 mM glucose, 2 mM $CaCl_2$ and 1 mM $MgCl_2$ and incubated at 34°C for 30 min.

Calcium imaging

Slices were moved to an imaging chamber containing aCSF positioned below a digital camera (ORCA-ER, Hamamatsu) mounted on an Olympus upright microscope (BX51WI). Micro-manager software (version 1.4) was used to control the microscope interface. Cells were imaged at 10X magnification (5 Hz; 200ms exposure time) with 470 nm excitation through a filter set (U-N41 017, E.X. 470 nm, B.S. 495 nm, E.M. 5, Olympus). Throughout the experiment, slices were superfused with oxygenated aCSF. Initially aCSF KCl concentration was set at physiological levels of 4mM. In order to measure the relationship between neuronal depolarization and changes in GCaMP6s fluorescence, aCSF KCl concentration was systematically increased to elicit increased neuronal depolarization. After an initial 5 min 4mM KCl baseline period, KCl concentration was increased to 10mM for 5 min, followed by 15mM for 5 min, and finally a return to 4mM baseline for 5 min.

Data analysis

Data analysis was performed as described previously (Chen et al., 2015). Individual regions of interest (ROIs) containing an identifiable cell nucleus were selected using the oval selection tool in ImageJ. Then, using the Plot Z axis Profile function in ImageJ, the mean gray value of each ROI was obtained for all frames ($F_{Cell\_Measured}$). Additionally, an estimate of neuropil fluorescence ($F_{Neuropil}$) was obtained by selecting the surrounding of the cell using the same procedures. The true fluorescence signal of each cell was then estimated using the function: $F_{Cell\_True(t)} = F_{Cell\_Measured(t)} - (F_{Neuropil(t)} \times r)$, with r = 0.7 (Chen et al., 2015). $F_{Cell\_True(t)}$ for each cell was then normalized to the median of the initial 5 min 4mM KCl baseline period. To establish the relationship between neuronal depolarization and GCaMP6s fluorescence, peak Fn (see below) averaged across cells in the final minute of the four KCl concentration conditions was compared for male and female GCaMP6s and control eGFP groups.

Fiber Photometry

Calcium imaging

Fiber photometry was conducted as described previously (Chen et al., 2015; Cui et al., 2013; Gunaydin et al., 2014). Briefly, using a fiber photometry setup (Figure 1B), a 473 nm laser diode excitation source (Omicron Luxx) was placed upstream to an optic chopper (Thorlabs) running at 400 Hz and then passed through a GFP excitation filter (Thorlabs). This signal was then reflected by a dichroic mirror (Semrock) into an optic fiber cable (Thorlabs). This cable was then linked to an optic fiber implant attached to the experimental mouse. Fluorescence emitted by GCaMP6s during the behavioral assay was filtered through a GFP emission filter (Thorlabs) and focused by a convex lens (Thorlabs) onto a photoreceiver (Newport 2151). The signal was then run into a lock-in amplifier (Stanford Research System), digitized by a data acquisition device (LabJack U6-Pro), and recorded on a computer at a 250 Hz sampling rate.

Optic fibers and cannulas were made using multimode fiber with a 400 μm core (Thorlabs FP400URT) that was stripped with a fiber stripper, lightly scored by an optic fiber scribe (Thorlabs S90R), and pulled by hand to create an optic fiber of appropriate length for implantation. The pulled end of each optic fiber was then inspected using a fiber microscope (Thorlabs FS200) and only fibers with > 90% smooth surface were used. Optic fibers were then inserted into a 2.5 mm ceramic ferrule (Thorlabs CF440-10), and fiber epoxy (Thorlabs F112) was applied to both ends and allowed to cure overnight. Finally, optic fibers were polished using a polishing disk (Thorlabs D50-FC) and calcined alumina lapping sheets (Thorlabs LF03P).

Prior to any behavioral testing, mice were habituated to the weight and feel of the optic fiber cable. The cable was attached to the optic fiber implants on the mice, and mice were allowed to move freely in their home cages during 4 separate 30 min habituation sessions.

Data analysis

Behavioral video files and fluorescence data were time-locked via a light flash present in both datasets that was initiated by a pulse generator (Doric OTPG-4). The raw fluorescence data was normalized to the median fluorescence of the 5 min baseline period before the entrance of any animal or object into the cage. For PETP, time zero was set to the start of a behavior or event of interest, and the median fluorescence during the time window 10 s prior to a behavioral event was used as the normalization factor to calculate change in fluorescence from baseline (F_n). For peri-event analysis of amplitude changes, the 95 percent peak fluorescence (peak F_n) was calculated and compared for the 10 s time window before and after a behavioral event. For mounting behavior, which transitions into intromission within 2-4 s, the time window from the initiation of mounting up until the start of intromission was used to calculate 95 percent peak F_n.

Chemogenetic inhibition

Chemogenetic inhibition studies were performed as described previously (Unger et al., 2015; Yang et al., 2017). CNO (Enzo) was dissolved in sterile saline at 5 mg/ml and kept as frozen aliquots. On the day of behavioral testing, CNO was freshly diluted in sterile saline to achieve a dose of 1 mg/kg. This dose of CNO was optimized for our studies and falls within the range used in previous studies (Unger et al., 2015; Yang et al., 2017). Experimental mice were injected intraperitoneally (IP) with CNO or sterile saline 30 min prior to behavioral assays. Mice were tested on each behavioral assay once each with CNO and saline, with the order of CNO and saline administration counterbalanced across animals.

Caspase-3 mediated ablation

Caspase-mediated ablation studies were performed as described previously (Unger et al., 2015; Yang et al., 2013). We virally expressed a Cre-dependent executioner caspase-3 in AB neurons in $Aro^{Cre/IPIN}$ and control Aro^{IPIN} mice, and waited $\geq$ 3 weeks to allow for maximal ablation of AB neurons. Only animals in which both the left and right BNSTpr showed cell loss > 50% compared to the number of aromatase cells in control Aro^{IPIN} mice were included for behavioral scoring and analysis. Animals were tested twice for each behavioral assay with their behavioral performance averaged across both assays for data presentation and analysis.

Optogenetic manipulation

Optic fibers and cannulas were made as described above for fiber photometry but with multimode fiber with a 200 μm core (Thorlabs FT200EMT) and 1.25 mm ceramic ferrules (Thorlabs CFLC230-10). All optogenetic stimuli were produced by a pulse generator (Doric OTPG-4) that triggered a blue light laser for ChR2 studies (473 nm; Opto Engine) and a yellow light laser for eNpHR3.0 studies (593.5 nm; Opto Engine). Laser illumination commenced as soon as an intruder was placed into the residents cage. For ChR2 studies, laser power was adjusted such that light exiting the optic fiber cable was 2mW. For persistent photostimulation, laser illumination was performed in cycles of 30 s light on and 30 s light off throughout the entire assay. For transient photostimulation, laser illumination was done continuously at 5Hz for the first 90 s of the assay, and then illumination was turned off for the rest of the assay. For eNpHR3.0 studies, laser power was adjusted such that light exiting the optic fiber cable was 6mW unless otherwise mentioned. For constant inhibition studies, laser illumination was on throughout the entire assay. For transient inhibition studies, laser illumination was continuously on for 90 s, and then illumination was switched off for the rest of the assay. For ChR2 and eNpHR3.0 studies, mice were tested on each assay once each with light illumination and no light illumination control, counterbalanced across animals. As with fiber photometry, prior to any behavioral testing, mice were habituated to the weight and feel of the optic fiber cable. Mice were given 4 separate 30 min habituation sessions.

Hormone priming

To control for cyclic hormone levels, all females used in mating assays were ovariectomized as described previously (Unger et al., 2015; Wu et al., 2009; Xu et al., 2012; Yang et al., 2013). To induce receptivity, females were hormonally primed by subcutaneous injection of 10 μg of 17-β-estradiol benzoate (EB, Sigma) suspended in sesame oil (48hrs before the assay), followed by 5 μg of EB (24hrs before the assay), and finally 50 μg of progesterone (Sigma) suspended in sesame oil (4-6hrs before the assay).

Hormone assays

Serum testosterone levels were measured using an ELISA kit (Cayman, #582701) (Yang et al., 2017) following the manufacturer's instructions.

Behavioral testing

All behavioral testing was initiated $\geq$ 1 hr after onset of the dark cycle and recorded using camcorders (Sony) under infrared illumination as described previously (Yang et al., 2013). Videos were played at 30 frames per second and manually annotated using custom software described previously (Wu et al., 2009; Xu et al., 2012; Yang et al., 2013). This permitted analysis of multiple parameters (including number, duration, latency, probability, and inter-event interval) of different behavioral routines. In particular, anogenital

investigation (sniff), mounting, repeated pelvic thrust (intromission), and ejaculation were scored for sexual behaviors. Receptivity index was calculated by dividing number of intromissions by number of mounts for each mouse. Lordosis events were defined by the display of a concave-arched back posture while braced on all four legs during a mount attempt. Lordosis Quotient (or Receptivity Quotient) was calculated as follows: (# lordosis events*100)/(# mounting events) (Thompson and Edwards, 1971). Aggression was scored as occurring when physical attacks (episodes of biting, wrestling, tumbling, chasing) were observed.

Both sexual and aggressive displays were annotated during female-male and male-male interactions. Mating assays during male-female interactions lasted for 30 min to enable display of different mating routines. Aggression assays (male-male; nursing female-intruder of either sex) were restricted to 15 min to allow fighting to occur but were short enough to preclude excessive attacks toward intruders. All behavioral studies were conducted using previously published procedures (Unger et al., 2015; Wu et al., 2009; Xu et al., 2012; Yang et al., 2013). The various behavioral assays used in the study are described briefly below.

Testing aggression in WT sexually naive males

For testing aggression in C57BL/6N males (the strain used in Remedios et al. [2017]), we purchased adult sexually naive males who had been group housed since weaning from Charles River; upon receipt of these males, we acclimated them to our reverse light cycle (lights-on at 1PM and lights-off at 1AM) for 14 days in group housing condition. However, males to be used as residents were acclimated to the reverse light cycle for 7 days, singly housed for 7 days, and then tested with group housed intruders of the same strain.

Sequence of behaviors for Figures 1, 2

To examine male AB neuronal activity during social interactions, we targeted a virally-encoded Cre-dependent GCaMP6s to and implanted an optic fiber over AB neurons of sexually naive $Aro^{Cre/IPIN}$ males that had been group housed by sex since weaning; we waited $\geq$ 4 weeks to allow for maximal viral expression. Prior to fiber photometry studies, these males were single housed for $\geq$ 7 days. Separate cohorts of males were assayed in their home cage during either a 15 min interaction with a WT group housed male or a 30 min interaction with a WT group housed hormonally primed female; for both of these cohorts, we assayed for changes in GCaMP6s fluorescence in multiple assays until the experimental male exhibited typical social displays, mating toward female intruder and aggression toward male intruder. Experimental males from both cohorts showed social behaviors even in the first assay (3/7 mated with females and 4/7 attacked males), and all males from both cohorts exhibited mating with females or aggression with males within 3 rounds of testing. Importantly, in no case was an experimental male being tested with an intruder of one sex ever tested with an intruder of the opposite sex; for example, none of the experimental males being tested with an intruder male underwent testing with a female, and they were therefore sexually naive at the time of euthanasia unless otherwise mentioned.

To examine female AB neuronal activity during maternal behaviors, we targeted a virally-encoded Cre-dependent GCaMP6s to and implanted an optic fiber over AB neurons of sexually naive $Aro^{Cre/IPIN}$ females that had been group housed by sex since weaning; we waited $\geq$ 4 weeks to allow for maximal viral expression. For assays of maternal behavior, a cohort of females was housed with WT male until visibly pregnant. Males were then removed ($\geq$5 days prior to fiber photometry studies), and females were allowed to deliver their litter. To assay pup retrieval, at days 2 and 4 after parturition, all pups were briefly removed from the cage and 4 pups were placed separately in the corners of the cage. Pup retrieval behavior was assayed for 5 min, allowing sufficient time for mothers to retrieve all pups. Following the assay, all pups were returned to the cage. To assay maternal aggression, pups at postnatal day 6, 8, 10, and 12 were removed, and a WT group-housed male or hormonally primed female intruder was inserted into the cage for 15 min. The order of the sex of the intruder (days 6 and 8 versus days 10 and 12) was counterbalanced across mice. Pups were returned to the cage following completion of the assay. On postnatal day 14, pups were removed briefly, and females were exposed for 3 min to a novel object (1.25" cubed wood block). Finally, on postnatal days 16, 18, and 20, pups were removed from the cage, and females were exposed for 3 min to a 1"x1" cotton swab wetted with urine or saline as described below.

To examine female AB neuronal activity during sexual behavior (Figures 2 and S2), we targeted a virally-encoded Cre-dependent GCaMP6s to and implanted an optic fiber over AB neurons of sexually naive $Aro^{Cre/IPIN}$ or $Vgat^{Cre}$ females that had been group housed by sex since weaning and removed their ovaries; we waited $\geq$ 4 weeks to allow for maximal viral expression. These females were single housed for $\geq$ 7 days prior to fiber photometry studies. To assay sexual behavior, these females were hormonally primed to be receptive and placed into the home cage of a WT sexually experienced male for 30 min. To examine the early response of sexually experienced estrus female AB neurons to the two sexes, these females were subsequently tested with group housed WT males or estrus females or wood block in 3 min encounters as described below for males.

Sequence of behaviors for Figure 3

To examine the early response of sexually naive male AB neurons to the two sexes, we targeted a virally-encoded Cre-dependent GCaMP6s to and implanted an optic fiber over AB neurons of a new cohort of sexually naive $Aro^{Cre/IPIN}$ males that had been group housed by sex since weaning; we waited $\geq$ 4 weeks to allow for maximal viral expression. Prior to fiber photometry studies, these males were single housed for $\geq$ 7 days. These males were exposed for 3 min on separate days in their home cage to a WT group housed hormonally primed receptive female, a WT group housed male, or wood block, with the order of the intruder assays counterbalanced across the 3 conditions.

To test whether sexual experience altered the response of AB neurons toward males and females, a subset of males used in the mating assays of Figure 2, which were now sexually experienced, were exposed for 3 min in their home cage, on separate days and in a counter-balanced manner, to a WT group housed male or receptive female intruder or novel object (wood block, 1.25" per side).

To test whether the loss of sexual motivation following Cx altered the response of AB neurons toward males and females, we expressed GCaMP6s as described in the next paragraph in another cohort of sexually naive males and assayed them using the same

3 min encounter paradigm described above prior to and ≥ 14 days following Cx. Cx males of this latter cohort were subsequently tested for ≥ 30 min in their home cage with WT receptive females for male-typical mating behaviors to confirm functional absence of circulating testosterone prior to euthanasia.

To examine the early response of sexually naive male AB neurons to pheromones or behaviorally salient odors, we expressed GCaMP6s in AB neurons as described above in another cohort of sexually naive $Aro^{Cre/IPIN}$ males and exposed them for 3 min on separate days in their home cage to a 1"x1" cotton swab wetted with 80 μl of undiluted urine from WT group housed C57BL/6J males, primed receptive C57BL/6J females, or saline; the order of the swab assays was counterbalanced across the 3 conditions. Urine was collected 3-6 hours prior to use and kept on ice until pipetted onto the swab. To test the selectivity of the response of male AB neurons to specific odors, we expressed GCaMP6s in AB neurons as described above in a different cohort of sexually naive $Aro^{Cre/IPIN}$ males and exposed them for 3 min on separate days in their home cage to cotton swabs wetted with 80 μL of 3μM PEA (Sigma) (Liberles, 2015), 20 μM cadaverine (Sigma) (Liberles, 2015), undiluted urine from males or females as described earlier in this paragraph, or saline in a counterbalanced manner. These males, who were still sexually naive, were subsequently Cx and used as described in the preceding paragraph.

To test the effects of chemogenetic inhibition of male AB neuronal activity on pheromone preference, we targeted a virally-encoded Cre-dependent DREADDi (hM4DGi) to AB neurons of sexually naive $Aro^{Cre/IPIN}$ males that had been group housed by sex since weaning; we waited ≥ 2 weeks to allow for maximal viral expression. Prior to pheromone preference assays, these males were single housed for ≥ 7 days. Males were tested on the pheromone preference assay once each with CNO and saline injected 30 min prior to the assay, with the order of CNO and saline administration counterbalanced across animals. During the preference assay, two 1"x1" cotton swabs (one wetted with 80 μl of undiluted WT group housed hormonally primed C57BL/6J female urine and the other wetted with 80 μl of undiluted WT group housed C57BL/6J male urine) were placed at opposite ends of their home cage. Mice were given 5 min to investigate the urine swabs. Duration, latency, and number of sniffs for each swab were scored. To test the effects of ablation of male AB neurons on pheromone preference, we targeted a virally-encoded Cre-dependent executioner caspase-3 to AB neurons of sexually naive $Aro^{Cre/IPIN}$ and control Aro^{IPIN} males, and waited ≥ 3 weeks to allow for maximal ablation of AB neurons. Prior to pheromone preference assays, these males were single housed for ≥ 7 days. Males were then tested on the pheromone preference assay twice, and their performance was averaged across the two trials.

Sequence of behaviors for Figure 4

To examine the impact of Trpc2-dependent signaling on pheromone preference, we single housed $Trpc2^{-/-}$ and $Trpc2^{+/-}$ males for ≥ 7 days and subsequently tested them on the 5 min pheromone preference assay twice with their performance averaged across the two trials. To examine the impact of Trpc2-dependent signaling on male AB neuronal activity, we targeted a virally-encoded Cre-dependent GCaMP6s to and implanted an optic fiber over AB neurons of sexually naive $Aro^{Cre/IPIN}$; $Trpc2^{-/-}$ males that had been group housed by sex since weaning; we waited ≥ 4 weeks to allow for maximal viral expression. Prior to fiber photometry studies, these males were single housed for ≥ 7 days. These males were first assayed using the 3 min urine swab encounter paradigm described above and then subsequently assayed using the 3 min intruder encounter paradigm described above. Finally, these males were assayed in their home cage during separate 30 min interactions with a WT group housed male and a WT group housed hormonally primed receptive female.

Sequence of behaviors for Figure 5

To test the effects of chemogenetic inhibition of male AB neuronal activity on mating behavior, we targeted a virally-encoded Cre-dependent DREADDi to AB neurons of sexually naive $Aro^{Cre/IPIN}$ males that had been group housed by sex since weaning; we waited ≥ 2 weeks to allow for maximal viral expression. Prior to mating assays, these males were single housed for ≥ 7 days. During the assay, a WT group-housed hormonally primed receptive female was inserted into the male's home cage for 30 min. Males were tested for mating behavior once each with CNO and saline injected 30 min prior to the assay, with the order of CNO and saline administration counterbalanced across animals. To test the effects of ablation of male AB neurons on mating behavior, we targeted a virally-encoded Cre-dependent executioner caspase-3 to AB neurons in $Aro^{Cre/IPIN}$ and control Aro^{IPIN} males, and waited ≥ 3 weeks to allow for maximal ablation of AB neurons. Prior to mating assays, these males were single housed for ≥ 7 days. Males were then tested on the 30 min mating assay twice with hormonally primed WT receptive females, and their performance was averaged across the two trials.

To test the effects of chemogenetic inhibition of female AB neuronal activity on sexual receptivity, we targeted a virally-encoded Cre-dependent DREADDi to AB neurons of sexually naive $Aro^{Cre/IPIN}$ females that had been group housed by sex since weaning and removed their ovaries; we waited ≥ 2 weeks to allow for maximal viral expression. During the assay, group housed experimental females were hormonally primed to be receptive and then inserted into the home cage of a WT singly housed sexually experienced male for 30 min. Females were tested for sexual receptivity once each with CNO and saline injected 30 min prior to the assay, with the order of CNO and saline administration counterbalanced across animals. To test the effects of ablation of female AB neurons on sexual receptivity, we targeted a virally-encoded Cre-dependent executioner caspase-3 to AB neurons in $Aro^{Cre/IPIN}$ and control Aro^{IPIN} females, removed their ovaries, and waited ≥ 3 weeks to allow for maximal ablation of AB neurons. Group housed females were then tested on the 30 min sexual receptivity assay twice as described above, and their performance was averaged across the two trials.

Sequence of behaviors for Figure 6

To test the effects of chemogenetic inhibition of male AB neuronal activity on aggression behavior, experimental $Aro^{Cre/IPIN}$ males previously tested for mating behavior (Figure 5) were assayed for territorial aggression behavior. During the assay, a WT group-housed male was inserted into the experimental male's home cage for 15 min. Males were tested for aggression behavior once each with CNO and saline injected 30 min prior to the assay, with the order of CNO and saline administration counterbalanced across animals. To test the effects of ablation of male AB neurons on aggression behavior, experimental $Aro^{Cre/IPIN}$ and control Aro^{IPIN} males previously tested for mating behavior (Figure 5) were assayed for territorial aggression behavior. Males were then tested on the 30 min territorial aggression assay twice, and their performance was averaged across the two trials.

To test the effects of chemogenetic inhibition of female AB neuronal activity on maternal behaviors, we targeted a virally-encoded Cre-dependent DREADDi to AB neurons of sexually naive $Aro^{Cre/IPIN}$ females that had been group housed by sex since weaning; we waited $\geq$ 2 weeks to allow for maximal viral expression. These females were housed with WT male until visibly pregnant. Males were then removed ($\geq$5 days prior to maternal behavior assays), and females were allowed to deliver their litter. Females were tested for each maternal behavior once each with CNO and saline injected 30 min prior to the assay, with the order of CNO and saline administration counterbalanced across animals. Pup retrieval assays as described above were conducted on days 3 and 5 after parturition. Percent retrieval, latency, and time to retrieve all pups were scored. On days 7 and 9 after parturition, pups were briefly removed from the cage, and a WT group housed male was inserted into the cage for 15 min. Following assays of maternal aggression, mothers were assayed for non-social behaviors. On days 11 and 13 after parturition, they were tested for anxiety-like behavior with the elevated plus maze. Females were placed in the center of an elevated plus maze facing the open arm at the start of the assay. Time spent in the closed or open arms during the 5 min assay was scored. On days 15 and 17 after parturition, females were tested for olfactory motivated behavior with a food finding assay. After being food deprived for 6hrs, females were inserted into a clean cage with a cracker (Cheez-It) buried under the bedding. Females were given 5 min to find the cracker at which time the assay ended. Latency to find the food was scored.

To test the effects of ablation of female AB neurons on maternal behaviors, we targeted a virally-encoded Cre-dependent executioner caspase-3 to AB neurons in $Aro^{Cre/IPIN}$ and control Aro^{IPIN} females, and waited $\geq$ 3 weeks to allow for maximal ablation of AB neurons. These females were housed with WT male until visibly pregnant. Males were then removed ($\geq$5 days prior to maternal behavior assays), and females were allowed to deliver their litter. These females were then tested twice for the maternal behaviors described above in the same order and on the same post-natal days as with chemogenetic inhibition studies. Their performance was averaged across the two trials.

Following tests of mating and aggression, experimental males and females were also assayed for performance in elevated plus maze, latency to find hidden food, and locomotor activity as described above as well as previously (Unger et al., 2015; Xu et al., 2012; Yang et al., 2013). Furthermore, changes in body weight subsequent to ablation of AB neurons was assessed by weighing mice immediately prior to stereotaxic surgery and again prior to perfusion at the conclusion of the behavioral experiments. Mice were given $\geq$ 1 days between each behavioral test.

Sequence of behaviors for Figure 7

To test the effects of optogenetic activation of male AB neuronal activity on mating and aggression behavior, we targeted a virally-encoded Cre-dependent ChR2 to AB neurons of sexually naive $Aro^{Cre/IPIN}$ males that had been group housed by sex since weaning and implanted optic fibers bilaterally over their BNSTpr; we waited $\geq$ 3 weeks to allow for maximal viral expression. Prior to behavioral assays, these males were single housed for $\geq$ 7 days. Males were tested, in a counter balanced order, on 30 min mating and 15 min aggression assays described above once each under light and no light conditions counterbalanced across animals. Laser illumination conditions are described above in the "Optogenetic manipulation" section. To test the effects of optogenetic activation of female AB neuronal activity on social interactions (Table S1), we targeted a virally-encoded Cre-dependent ChR2 to AB neurons of sexually naive $Aro^{Cre/IPIN}$ females that had been group housed by sex since weaning, removed ovaries, implanted optic fibers bilaterally over their BNSTpr, and waited $\geq$ 3 weeks to allow for maximal viral expression. Prior to behavioral assays, these females were single housed for $\geq$ 7 days. Females were hormonally primed on the day of testing, and a WT group housed hormonally primed female was inserted into the cage for 30 min or the experimental females were inserted into the cage of WT sexually experienced male for 30 min in a counterbalanced manner. Females tested on the behavioral assay once each under persistent light and no light conditions counterbalanced across animals.

To test the effects of optogenetic inhibition of male AB neuronal activity on mating behavior, we targeted a virally-encoded Cre-dependent eNpHR3.0 to AB neurons of sexually naive $Aro^{Cre/IPIN}$ males that had been group housed by sex since weaning and implanted optic fibers bilaterally over their BNSTpr; we waited $\geq$ 3 weeks to allow for maximal viral expression. Prior to behavioral assays, these males were single housed for $\geq$ 7 days. Males were tested on the 30 min mating assay described above once each under light and no light conditions counterbalanced across animals. Persistent and transient laser illumination conditions used are described above in the "Optogenetic manipulation" section unless mentioned otherwise.

QUANTIFICATION AND STATISTICAL ANALYSIS

Calcium imaging data, behavioral video recordings, and histological samples were analyzed blind to relevant variables, including sex, genotype, CNO administration, light illumination conditions, surgical procedure, and virus injected. Statistical analysis was performed using GraphPad PRISM (GraphPad Software). To compare categorical data including percentage of mice displaying a behavior, Fisher's exact test was performed from a 2x2 contingency table. To compare non-categorical data, including 95 percent peak F_n, duration of sniffing swabs and various behavioral paraameters, we first determined if the data values were from a normal distribution using the D'Agostino-Pearson omnibus normality test. In experiments with paired samples, we used a paired t test or repeated-measures ANOVA for parametric data and a Wilcoxon matched-pairs signed rank test or Friedman test for non-parametric data. In all other experiments, we used a t test or ANOVA for parametric data and a Mann-Whitney or Kruskal-Wallis test for non-parametric data. All multiple comparisons were corrected for using Bonferroni corrections.

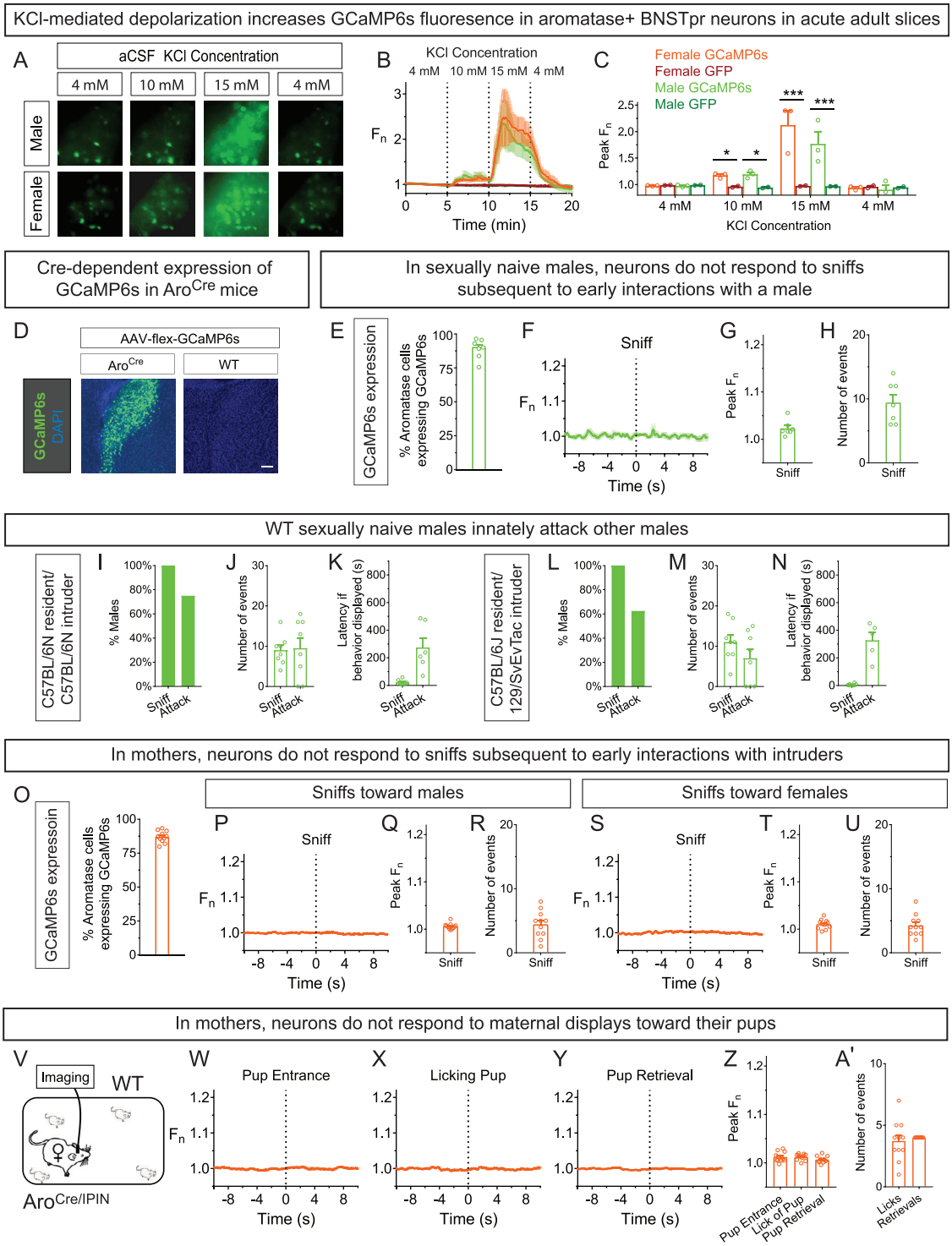

Figure S1. AB Neurons Are Not Active during Specific Aspects of Innate Displays of Male Territorial Aggression and Maternal Behaviors, Related to Figure 1

(A-C) Imaging GCaMP6s fluorescence in AB neurons in acute slice from adult *Aro*^{Cre} mice. Significant increase in fluorescence at 10mM and 15mM of KCl compared to EGFP expressing control AB neurons that subsides to baseline at 4mM KCl. For experimental and control slices, virally encoded, Cre-dependent GCaMP6s and EGFP, respectively, were delivered to the BNST of *Aro*^{Cre} mice.

(D) GCaMP6s is not detectable in WT males following injection of AAV encoding Cre-dependent GCaMP6s. Scale bar = 100 μm.

(E-H) Fiber photometry of AB neurons in singly housed *Aro*$^{Cre/IPIN}$ male interacting with group housed WT intruder male.

(legend continued on next page)

(E) Percent nuclear β-galactosidase+ AB neurons that express GCaMP6s in $Aro^{Cre/IPIN}$ males following viral delivery of Cre-dependent GCaMP6s.
(F,G) No significant change in GCaMP6s fluorescence during sniffing events displayed after the early interaction with an intruder.
(H) Number of such sniffing events in the assay.
(I-K) Singly housed, sexually naive WT C57BL/6N males attack a WT group housed intruder male (also C57BL/6N) in their cage multiple times; this strain was used recently to examine neural coding of male aggression in sexually naive and experienced males (Remedios et al., 2017).
(L-N) Singly housed, sexually naive WT C57BL/6J males attack a WT group housed intruder male (129/SvEvTac) in their cage multiple times. The WT residents are in the same background as our experimental $Aro^{Cre/IPIN}$ males.
(O-A') Fiber photometry imaging of AB neurons in $Aro^{Cre/IPIN}$ nursing female interacting with group housed intruder WT male (O-Q) or female (R-T), or her pups (U-Z).
(O) Percent nuclear β-galactosidase+ AB neurons that express GCaMP6s in $Aro^{Cre/IPIN}$ nursing females following viral delivery of Cre-dependent GCaMP6s.
(P,Q,S,T) No significant change in GCaMP6s fluorescence during sniffing events displayed after the early interaction with an intruder.
(R,U) Number of such sniffing events in the assay.
(V-Z) No significant increase in GCaMP6s fluorescence when pups are inserted back into cage, or when the mother licks her pups or retrieves them to the nest.
(A') Number of lick and retrieval events per assay.
Mean ± SEM n = 3 (A-C, each sex expressing GCaMP6s), 2 (A-C, each sex expressing GFP), 2 (D, WT), 7 (E-H), 8 (I-N, each strain), 11 (O-A'). *$p < 0.05$, ***$p < 0.001$.

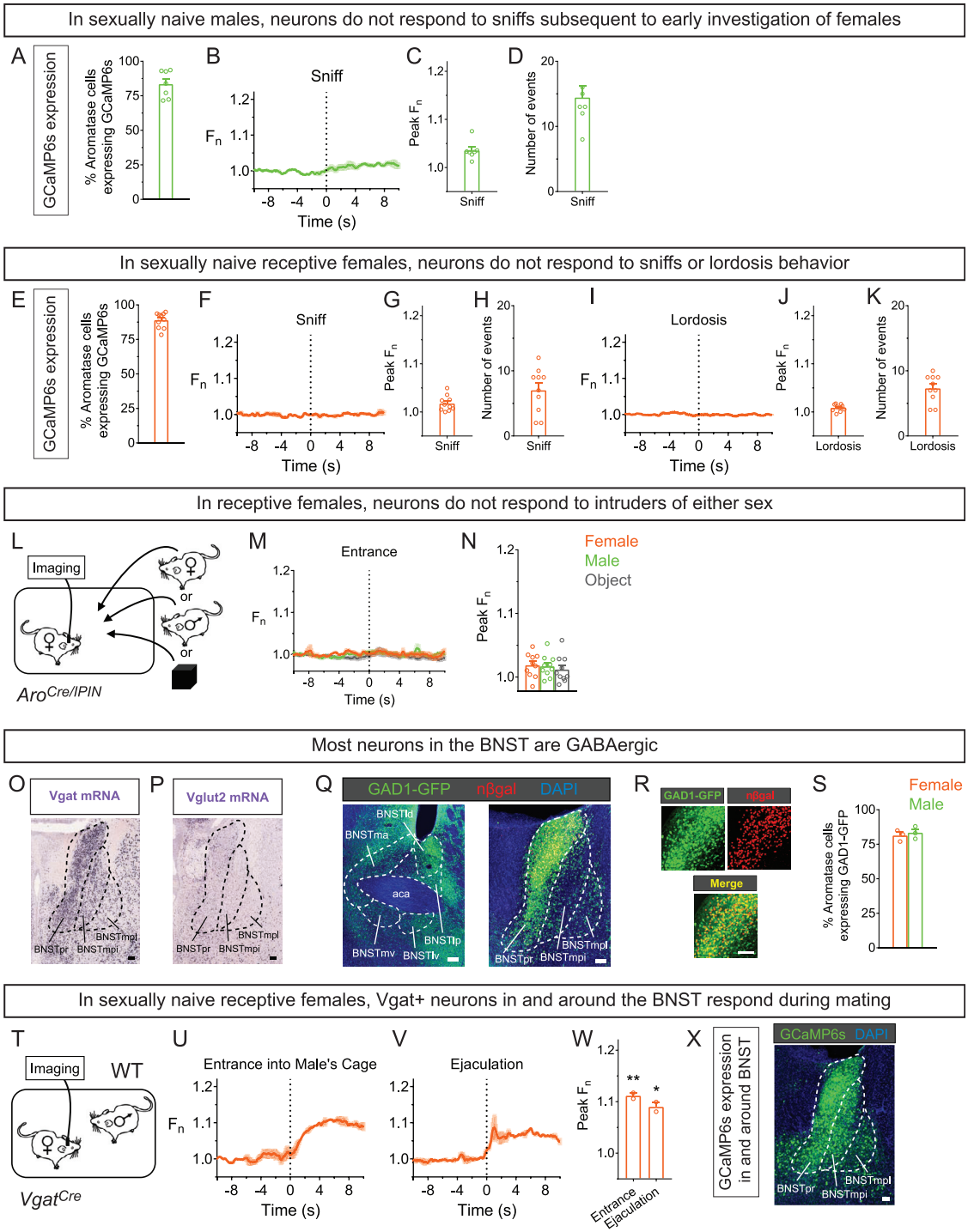

Figure S2. AB Neurons Are Not Activated with Sniffing Behavior Observed during Sexual Behavior, Related to Figure 2

(A-D) Fiber photometry of AB neurons in singly housed *Aro*$^{Cre/IPIN}$ male interacting with group housed WT receptive female inserted into his cage.

(A) Percent nuclear β-galactosidase+ AB neurons that express GCaMP6s in *Aro*$^{Cre/IPIN}$ males following viral delivery of Cre-dependent GCaMP6s.

(B,C) No significant change in GCaMP6s fluorescence during sniffing events displayed after the early interaction with an intruder.

(D) Number of such sniffing events in the assay.

(E-K) Fiber photometry of AB neurons in sexually naive receptive *Aro*$^{Cre/IPIN}$ females interacting with WT male after being inserted into his cage.

(E) Percent nuclear β-galactosidase+ AB neurons that express GCaMP6s in *Aro*$^{Cre/IPIN}$ females following viral delivery of Cre-dependent GCaMP6s.

(F,G) No significant change in GCaMP6s fluorescence during sniffing events displayed after the early interaction with an intruder.

(legend continued on next page)

(H) Number of such sniffing events in the assay.
(I,J) No significant change in GCaMP6s fluorescence during lordosis.
(K) Number of lordosis events in the assay.
(L-N) No significant change in GCaMP6s fluorescence in sexually receptive females upon insertion of male, female, or object into her home cage.
(O-S) Neurotransmitter characterization of AB neurons.
(O,P) Coronal sections through adult male BNST showing *in situ* hybridization for Vgat and Vglut2 mRNA (Ng et al., 2009) (Original images obtained from Allen Institute and annotated for presentation here). BNSTpr, BNSTmpi (medial division, posterointermediate part of BNST), and BNSTmpl (medial division, posterolateral part of BNST) outlined. Data taken from Allen mouse brain atlas (Vglut2: Experiment 73818754, section 38; Vgat: Experiment 72081554, section 38).
(Q) Immunolabeling for EGFP (Gad1) and nuclear β-galactosidase (aromatase) in $Aro^{IPIN};Gad1^{EGFP}$ adult mouse shows many GABAergic neurons in various subdivisions of the BNST whereas aromatase expression (yellow cells) appears limited to BNSTpr. BNSTld (lateral division, dorsal part of BNST), BNSTlp (lateral division, posterior part of BNST), BNSTlv (lateral division, ventral part of BNST), BNSTma (medial division, anterior part of BNST), and BNSTmv (medial division, ventral part of BNST).
(R,S) Immunolabeling for EGFP (Gad1) and nuclear β-galactosidase (aromatase) in $Aro^{IPIN};Gad1^{EGFP}$ adult mouse shows that the majority of AB neurons are GABAergic (Gad1+) in both sexes.
(T-X) Fiber photometry of AB neurons in sexually naive receptive $Vgat^{Cre}$ females interacting with WT male after being inserted into his cage.
(U-W) Significant increase in GCaMP6s fluorescence upon entry into male's cage and during ejaculation.
(**X**) Extensive expression of GCaMP6s in multiple BNST compartments and beyond, consistent with widespread expression of Gad1 and Vgat within the BNST.
Mean ± SEM n = 7 (A-D), 10 (E-N), 3 (Q-S, each sex), 2 (T-X). *$p < 0.05$, **$p < 0.01$. Scale bars = 100μm.

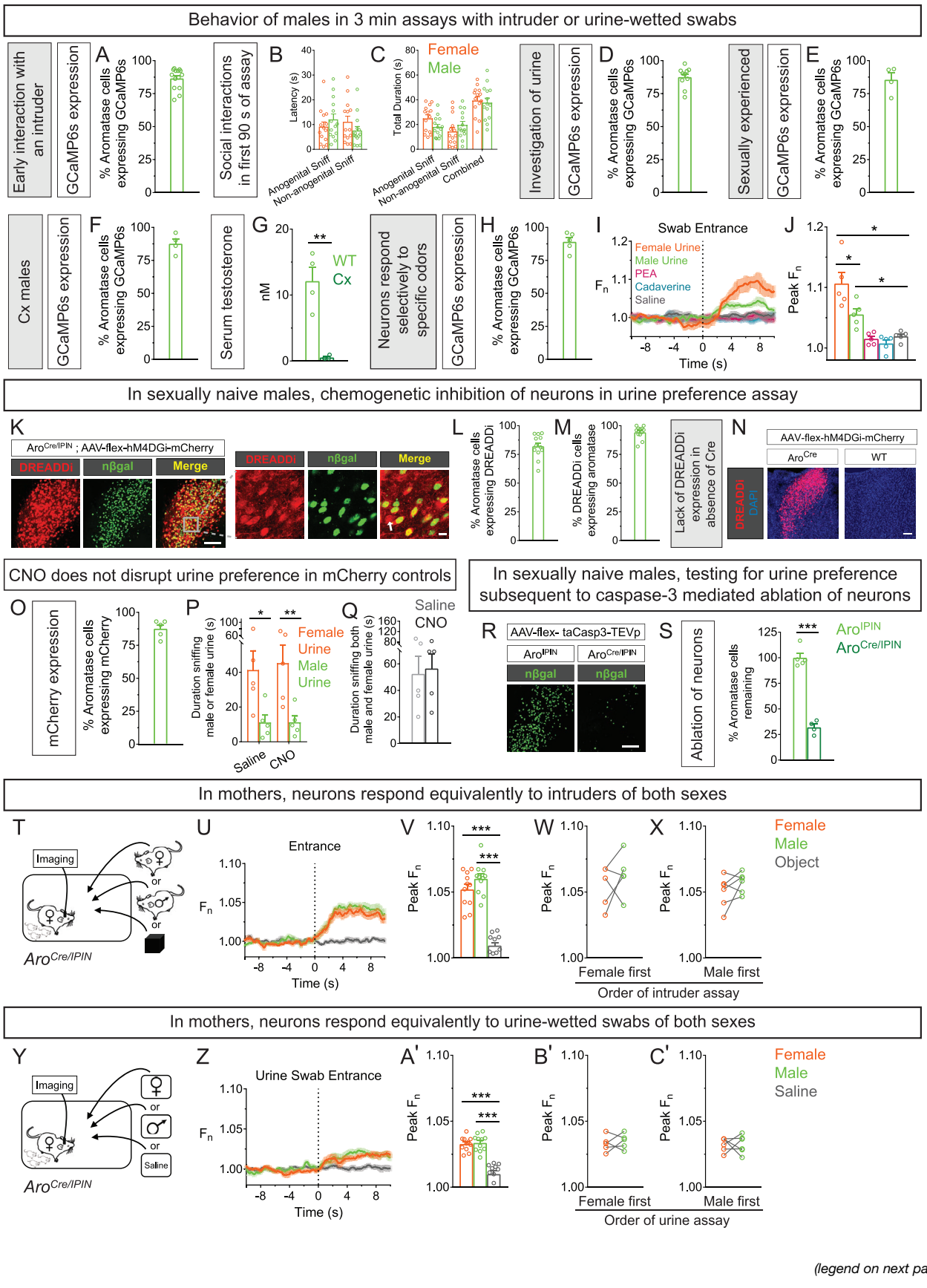

(legend on next page)

Figure S3. AB Neurons Are Activated during Early Interactions with an Intruder and by Pheromones in Urine, Related to Figure 3

(A-C) Fiber photometry of AB neurons in singly housed *Aro*$^{Cre/IPIN}$ male interacting for 3 min with group housed WT male or receptive female inserted into his cage.

(A) Percent nuclear β-galactosidase+ AB neurons that express GCaMP6s in *Aro*$^{Cre/IPIN}$ males following viral delivery of Cre-dependent GCaMP6s.

(B,C) No difference in latency to interact or in total duration of interactions with female or male intruder.

(D) Percent nuclear β-galactosidase+ AB neurons that express GCaMP6s in singly housed *Aro*$^{Cre/IPIN}$ males following viral delivery of Cre-dependent GCaMP6s. Fiber photometry was performed in these males as they interacted for 3 min with swab wetted with saline or male or female urine.

(E,F) Percent nuclear β-galactosidase+ AB neurons that express GCaMP6s in *Aro*$^{Cre/IPIN}$ males following viral delivery of Cre-dependent GCaMP6s in gonadally intact sexually experienced males (E) or Cx males (F).

(G) Serum testosterone in gonadally intact WT males or Cx *Aro*$^{Cre/IPIN}$ males.

(H) Percent nuclear β-galactosidase+ AB neurons that express GCaMP6s in *Aro*$^{Cre/IPIN}$ males following viral delivery of Cre-dependent GCaMP6s.

(I,J) Significantly larger change in GCaMP6s fluorescence upon insertion of swab wetted with urine from female compared to male. Urine wetted swabs elicited larger response compared to PEA, cadaverine, and saline.

(K-M) Coronal section through BNSTpr of *Aro*$^{Cre/IPIN}$ male immunolabeled for mCherry (DREADDi) and nuclear β-galactosidase (aromatase) visualized at lower magnification in left panels (scale bar = 100 μm) and at higher magnification in insets on right (scale bar = 10 μm; arrow shows occasional DREADDi+ neuron that does not express detectable level of nuclear β-galactosidase). Most AB neurons express DREADDi following viral delivery of Cre-dependent DREADDi:mCherry (L). Vast majority of DREADDi+ cells express aromatase (nuclear β-galactosidase) (M).

(N) mCherry is not detectable in WT males following injection of AAV encoding Cre-dependent DREADDi (fused to mCherry). Scale bar = 100 μm.

(O-Q) Specificity of CNO action. Virally encoded Cre-dependent mCherry was expressed in AB neurons of *Aro*$^{Cre/IPIN}$ males who were then subjected to urine swab preference test. Most AB neurons express mCherry (O), and CNO does not alter performance in sexual preference for female pheromones (P) or in total time spent sniffing (Q).

(R,S) Extent of ablation of AB neurons following expression of virally encoded, Cre-dependent caspase-3 in *Aro*$^{Cre/IPIN}$ and control *Aro*^{IPIN} males. Coronal sections indicates extensive loss of these cells in experimental males, which was assessed by quantifying nuclear β-galactosidase+ neurons in BNSTpr. Scale bar = 100 μm.

(T-C') Fiber photometry of AB neurons in *Aro*$^{Cre/IPIN}$ nursing females interacting for 3 min with an intruder or novel object (T-X) or swab wetted with urine or saline (Y-C').

(U,V) Significant increase in GCaMP6s fluorescence upon entry of intruder of either sex, and this increase is also significantly different from insertion of novel object.

(W,X) No difference in GCaMP6s fluorescence between entry of male or female intruder irrespective of the order of insertion.

(Z,A') Significant increase in GCaMP6s fluorescence upon insertion of swab wetted with female or male urine, and this increase is also significantly different from insertion of swab wetted with saline.

(B',C') No difference in GCaMP6s fluorescence between entry of male or female urine wetted swab, irrespective of the order of insertion.

Mean ± SEM n = 14 (A-C), 10 (D), 4 (E-G), 5 (H-J), 12 (K-M), 2 (N, WT), 5 (O-Q), 5 (R,S, *Aro*^{IPIN}), 4 (R,S, *Aro*$^{Cre/IPIN}$), 11 (T-C'). *$p < 0.05$, **$p < 0.01$, ***$p < 0.001$.

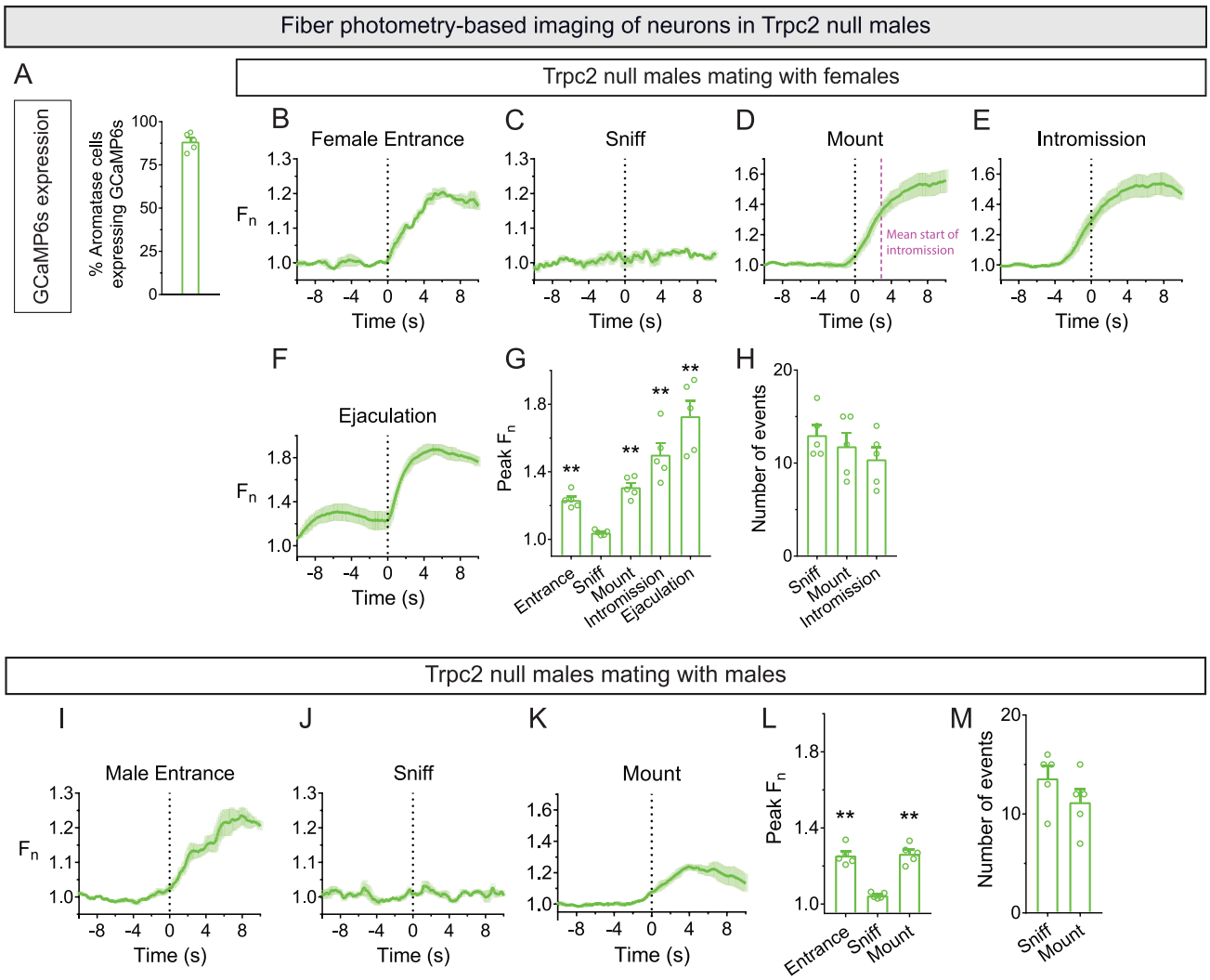

Figure S4. Activation of AB Neurons in *Aro*$^{Cre/IPIN}$;*Trpc2*$^{-/-}$ Males during Sexual Behavior, Related to Figure 4

(A) Percent nuclear β-galactosidase+ AB neurons expressing GCaMP6s.

(B-H) Changes in GCaMP6s fluorescence when singly housed mutant male mates with receptive WT female intruder.

(B-G) Significant increase in GCaMP6s fluorescence from baseline upon entry of female, when he mounts, intromits, and ejaculates, but not when he sniffs female following early interactions.

(H) Number of sniff, mounting, and intromission events per assay.

(I-M) Changes in GCaMP6s fluorescence when singly housed mutant male mates with group housed WT male intruder.

(I-L) Significant increase in GCaMP6s fluorescence from baseline upon entry of male, and when the mutant mounts him but not when he sniffs the intruder following early interactions.

(M) Number of sniff and mounting events per assay.

Mean ± SEM n = 5. **p < 0.01.

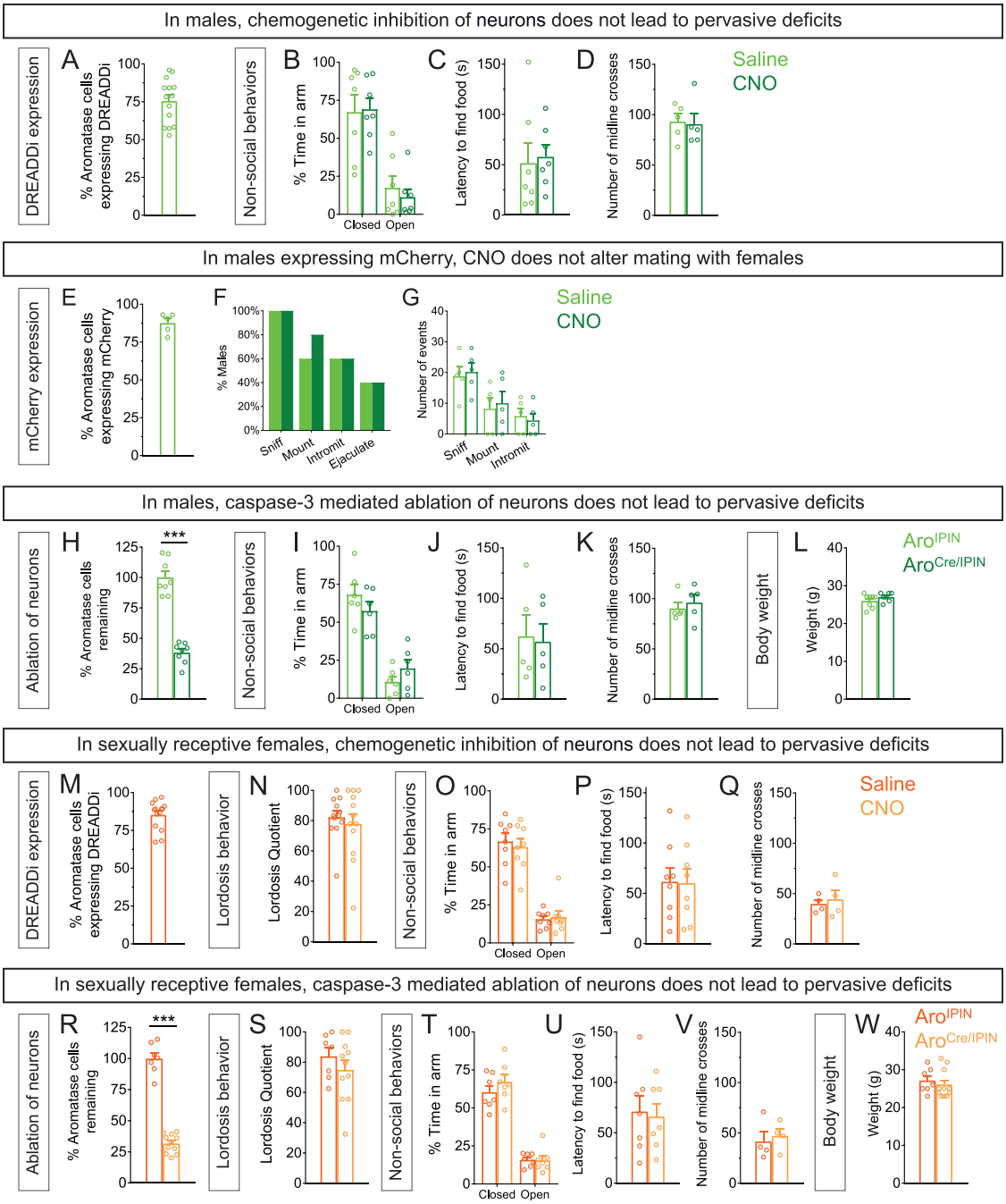

Figure S5. Functional Manipulation of AB Neurons Does Not Lead to Pervasive Deficits, Related to Figure 5

(A-D) mCherry (DREADDi) is expressed in the majority of nuclear β-galactosidase+ AB neurons of *Aro*$^{Cre/IPIN}$ males (A), but CNO does not alter performance in elevated plus maze (B), latency to find hidden food (C), or locomotor activity as assessed by midline crosses.

(E-G) mCherry (control) is expressed in the majority of nuclear β-galactosidase+ AB neurons of *Aro*$^{Cre/IPIN}$ males (E), but CNO does not alter performance in male sexual behavior (F,G).

(H-L) The majority of AB neurons is ablated following viral delivery of Cre-dependent caspase-3 in *Aro*$^{Cre/IPIN}$ males, as assessed by immunolabeling for β-galactosidase (H). Such ablation does not alter performance in elevated plus maze (I), latency to find hidden food (J), locomotor activity (K), and body weight (L).

(M-Q) mCherry (DREADDi) is expressed in the majority of nuclear β-galactosidase+ AB neurons of *Aro*$^{Cre/IPIN}$ females (M), but CNO does not alter performance in lordosis (N), elevated plus maze (O), latency to find hidden food (P), or locomotor activity (Q).

(legend continued on next page)

(R-W) The majority of AB neurons is ablated following viral delivery of Cre-dependent caspase-3 in $Aro^{Cre/IPIN}$ females, as assessed by immunolabeling for β-galactosidase (R). Such ablation does not alter performance in lordosis (S), elevated plus maze (T), latency to find hidden food (U), locomotor activity (V), and body weight (W).

Mean ± SEM n = 14 (A), 7 (B,C), 5 (D), 5 (E-G), 8 (H,L, each genotype), 6 (I, each genotype), 5 (J,K, each genotype), 14 (M), 12 (N), 8 (O,P), 4 (Q), 7 (R,S,W, Aro^{IPIN}), 11 (R,S,W, $Aro^{Cre/IPIN}$), 7 (T,U, each genotype), 4 (V, each genotype). ***$p < 0.001$.

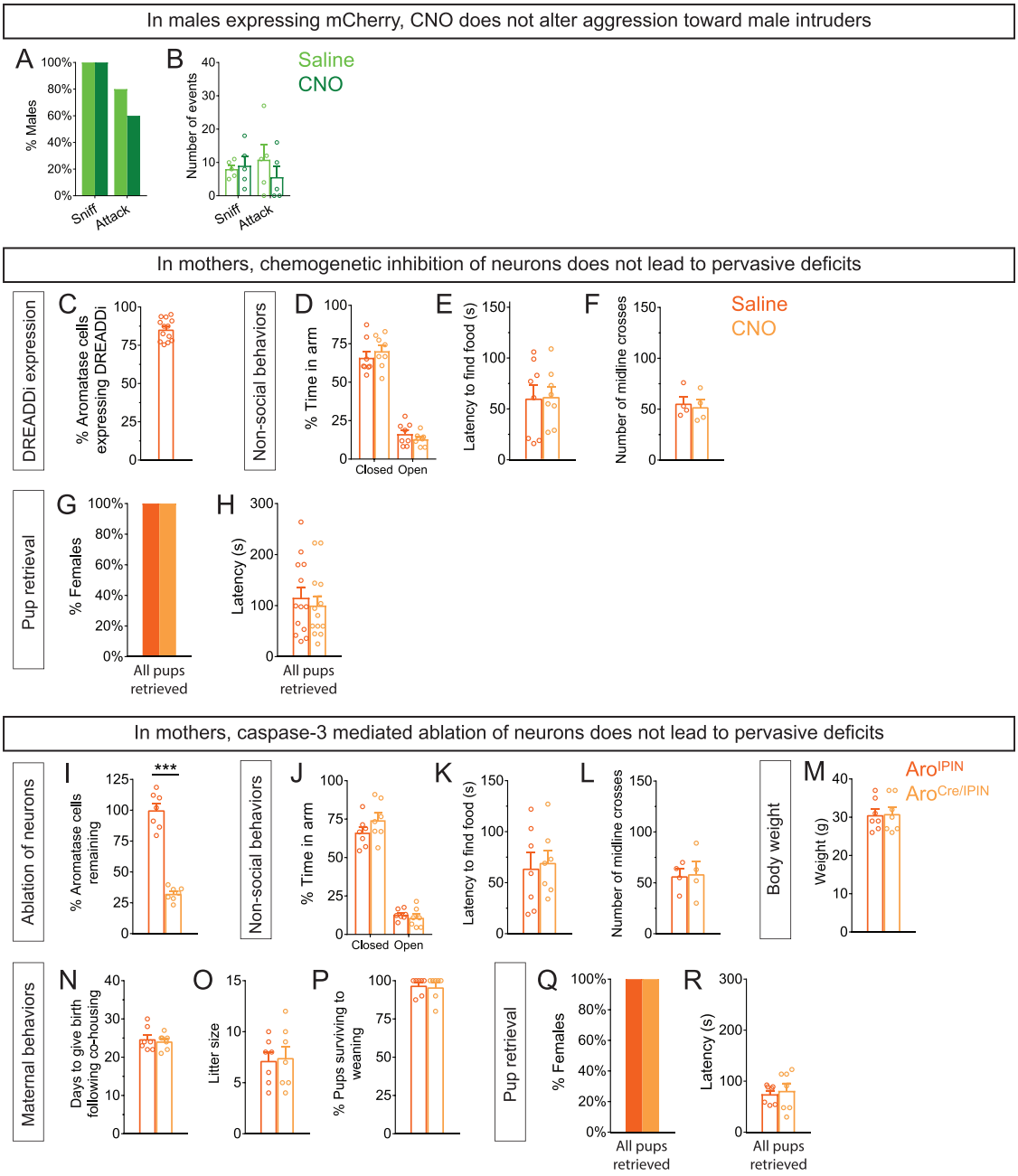

Figure S6. Specificity of Functional Role of AB Neurons, Related to Figure 6

(A,B) In control *Aro*$^{Cre/IPIN}$ males expressing mCherry instead of DREADDi, CNO does not alter male aggressive behavior. Same males as shown in Figure S5E-G.

(C-H) mCherry (DREADDi) is expressed in the majority of nuclear β-galactosidase+ AB neurons of *Aro*$^{Cre/IPIN}$ nursing females (C), but CNO does not alter performance in elevated plus maze (D), latency to find hidden food (E), locomotor activity (F), or pup retrieval (G,H).

(I-R) The majority of AB neurons is ablated following viral delivery of Cre-dependent caspase-3 in *Aro*$^{Cre/IPIN}$ nursing females, as assessed by immunolabeling for β-galactosidase (I). This does not alter performance in elevated plus maze (J), latency to find hidden food (K), locomotor activity (L), or body weight (M).

Such ablation also does not alter sexual behavior, fertility, and long term care of pups as assessed by time to deliver pups following co-housing with WT male (N), litter size at birth (O), and percent pups surviving to weaning (P). Ablation of AB neurons also did reduce pup retrieval (Q,R).

Mean ± SEM n = 5 (A,B), 13 (C,G,H), 8 (D,E), 4 (F), 7 (I-K, M-R, each genotype), 4 (L, each genotype). ***p < 0.001.

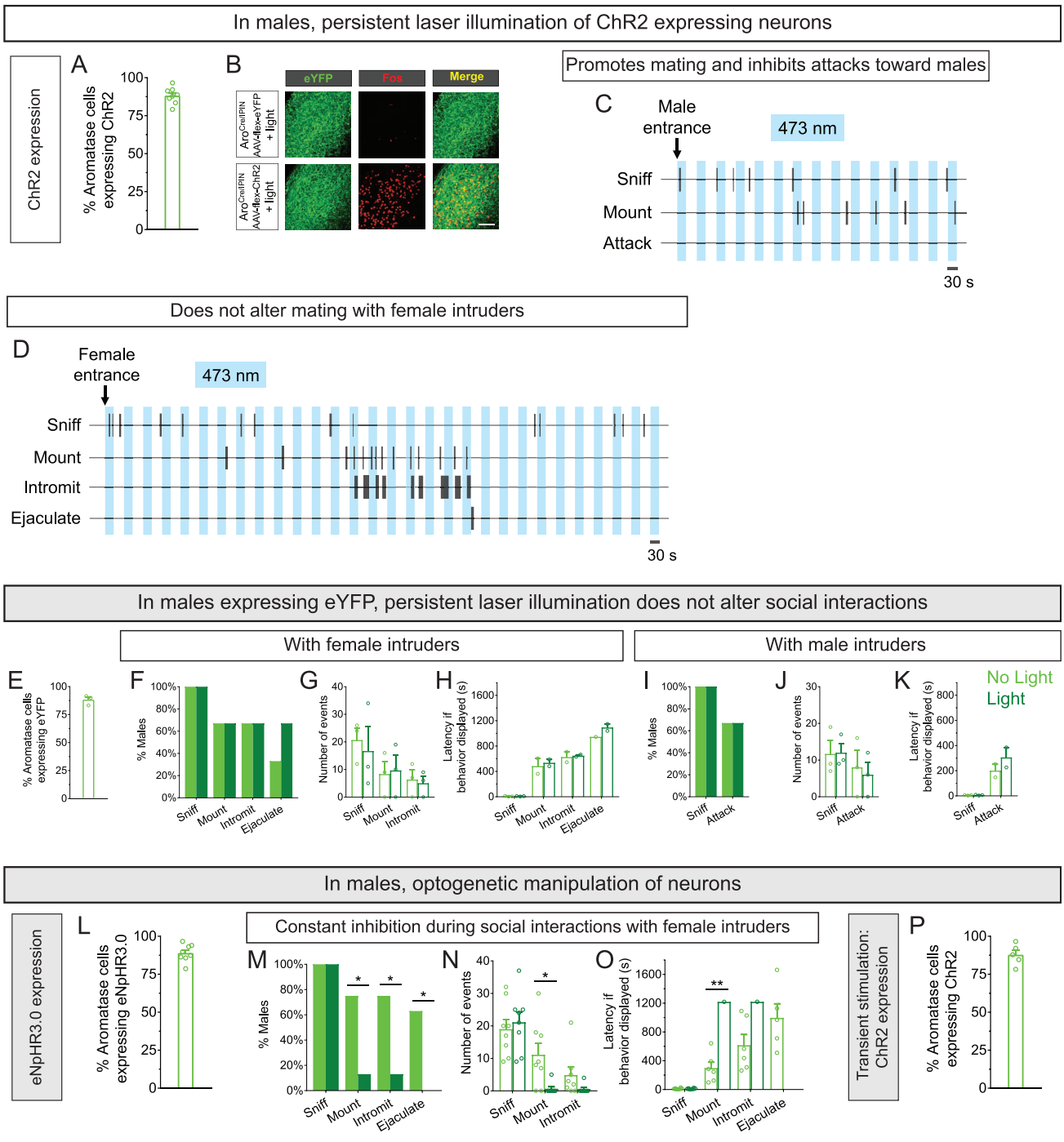

Figure S7. Optogenetic Manipulation of Male AB Neurons during Social Interactions, Related to Figure 7

(A-D) Persistent optogenetic stimulation of male AB neurons induces Fos and biases the male to initiate male-typical sexual behavior.

(A) Most nuclear β-galactosidase+ AB neurons express EYFP (ChR2).

(B) Coronal sections through BNSTpr of *Aro*$^{Cre/IPIN}$ male showing Fos induction in cells expressing ChR2 (bottom row) but not control fluorescent protein reporter upon laser illumination.

(C) Laser illumination inhibits experimental resident male from attacking a group housed WT male intruder and induces him to mount the intruder. Neither sniffing nor mounting are time-locked to stimulation epochs (blue columns) of 30 s duration. Entire 15 min encounter shown.

(D) Laser illumination does not alter experimental resident male sexual displays to a WT receptive female. Entire 30 min encounter shown.

(E-K) Optogenetic stimulation of AB neurons expressing virally encoded Cre-dependent EYFP in *Aro*$^{Cre/IPIN}$ males does not alter displays of mating with a WT receptive female (E-H) or aggression toward a group housed WT male intruder (I-K).

(legend continued on next page)

(L-O) Optogenetic inhibition of AB neurons inhibits male sexual behavior toward WT receptive female intruder. Viral delivery of Cre-dependent eNpHR3.0 leads to expression of eNpHR3.0 in the majority of these neurons in $Aro^{Cre/IPIN}$ males (L). Continous laser illumination reduces percent males mounting or intromitting and eliminates ejaculation (M), reduces mount number per assay (N), and significantly increases latency to start mounting (O).
(P) Viral delivery of Cre-dependent ChR2 leads to expression in the majority of AB neurons in $Aro^{Cre/IPIN}$ males.
Mean ± SEM n = 8 (A-D), 3 (E-K), 8 (L-O), 5 (Q). *$p < 0.05$, **$p < 0.01$. Scale bar = 100μm.